VYSOKÉ UČENÍ TECHNICKÉ V BRNĚ
BRNO UNIVERSITY OF TECHNOLOGY

FAKULTA INFORMAČNÍCH TECHNOLOGIÍ
ÚSTAV INTELIGENTNÍCH SYSTÉMŮ

FACULTY OF INFORMATION TECHNOLOGY
DEPARTMENT OF INTELLIGENT SYSTEMS

LIVENESS DETECTION OF A FINGER BASED ON CHANGES OF PAPILLARY LINES

DIPLOMOVÁ PRÁCE
MASTER'S THESIS

AUTOR PRÁCE
AUTHOR

BC. MICHAL LICHVÁR

BRNO 2008

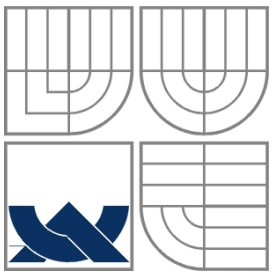

VYSOKÉ UČENÍ TECHNICKÉ V BRNĚ
BRNO UNIVERSITY OF TECHNOLOGY

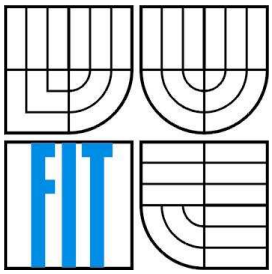

FAKULTA INFORMAČNÍCH TECHNOLOGIÍ
ÚSTAV INTELIGENTNÍCH SYSTÉMŮ

FACULTY OF INFORMATION TECHNOLOGY
DEPARTMENT OF INTELLIGENT SYSTEMS

DETEKCE ŽIVOSTI PRSTU NA ZÁKLADĚ ZMĚN PAPILÁRNÍCH LINIÍ

LIVENESS DETECTION OF A FINGER BASED ON CHANGES OF PAPILLARY LINES

DIPLOMOVÁ PRÁCE

MASTER'S THESIS

AUTOR PRÁCE
AUTHOR

BC. MICHAL LICHVÁR

VEDOUCÍ PRÁCE
SUPERVISOR

Ing. Martin Drahanský, Ph.D.

BRNO 2008

Here comes the original paper with the tasks.

Here come the license conditions.

Abstract

There are several frauds against biometric systems (BSs) and several techniques exist to secure BSs against these frauds. One of the techniques is liveness detection. To fool fingerprint sensors, latent fingerprints, dummy fingers and wafer-thin layer attached to the finger are being used. Liveness detection is being used also when scanning fingerprints. Several different characteristics of the live finger can be used to detect liveness, for example sweat, conductivity etc. In this thesis, new approach is examined. It is based on the expandability of the finger as an effect of heartbeats/pulsation. As the skin is expanding, also the distances between papillary lines are expanding. Whole finger expands approximately in range of $4{,}5\mu m$, the distance between two neighbor papillary lines in $0{,}454\mu m$. This value collides with wavelength of blue and green light. The result from this work is following. The resolution of the capturing device is not high enough to capture the expandability on distance between two neighbor papillary lines. Also, because of collision with wavelength, the diffraction effect is presented and the result images are influenced by this error.

Keywords

papillary lines, liveness detection, expandability of the skin, optical fingerprint sensor, frauds against biometric systems, optical lens parameters for capturing fingerprints.

Citation

Bc. Michal Lichvár: Liveness detection of a finger based on changes of papillary lines, diploma thesis, Brno, FIT BUT in Brno, 2008

Liveness detection of a finger based on changes of papillary lines

Declaration

I herebly declare that this paper is my original authorial work, which I have worked on my own under supervision of Dipl.-Ing. Martin Drahanský, Ph.D.
Further information was provided by mjr. Ing. Dr. Martin Řehoř
All sources, references and literature used or excerpted during elaboration of this work are properly cited and listed with complete references to relevant source.

……
Michal Lichvár
5/17/2008

Acknowledgements

I am very thankful to my adviser, Dipl. Ing. Martin Drahanský, Ph.D., for his help and wise guidance. In addition, I would like to thank mjr. Ing. Dr. Martin Řehoř for his useful information and patience with my basic questions. My friends and relatives also deserve thanks for their corrections and support.

Contents

1 Introduction

Since the beginning of mankind, people try to protect what they possess, whether it is information or property. Each protection system is secure only for a while, until it has been overrun. Therefore, the levels of security have to be still developed as the frauds and attackers are more sophisticated. One way of increasing the system security is the enhancement of the existing mechanism. The other is addition of some new security component, such as personal identification through its identity.

Identity is something, what we and only we have, it defines us; it is our human being. For determination of someone's identity, several biometric systems are used. They are based on unique physical or behavioral properties of human being.

Despite various biometric technologies exist, they have very similar operating model. First, the user has to enroll to the system, when the first measurement is made. During this process, user is registered and his biometric sample, known also as a master template, is processed and stored. Once the user's template is stored, it could be used for purpose of identification or verification.

During identification and verification, biometric system (BS) measures and processes a biometric sample to retrieve characteristics. The characteristics of the sample are then compared with all master templates and one master template, respectively. The result of comparison process is a matching score. This score is then threshold and the BS returns the final positive or negative decision.

BSs are divided in two groups based on the used biometric characteristic. The first ones use the physical characteristic, such as fingerprints, face or hand geometry, iris or retina pattern, DNA etc. The second group consists of voice recognition, keystroke or signature dynamics. These are called behavioral characteristics.

BSs are used in two main fields. First is the forensic and criminalistic area, where the biometric sample helps to identify the persons and capture the criminals. The second, becoming still more popular, is the security usage of BS. They are used to access bank accounts (ATMs with retina scanners in Japan), to login into computer (e.g. fingerprint scanner embedded in notebook) or to access secret zones.

One way, how to get through these systems, is a forgery of someone's identity. This is not a new issue, stealing, replacing or faking identity were used by spies also in ancient times. However, for a fraud of BS you need to use special techniques. And of course, you need to have some technique in advanced to detect these frauds. This could be done using liveness detection, especially when BS is using physical characteristic. While the behavioral characteristic assumes liveness to obtain sample, physical characteristic is static, so it could be forged e.g. by static image. Therefore, some dynamic attribute should extend the BS to prove liveness (e.g.: while scanning retina, the iris reaction to flashlight is measured).

1.1 Goals

The main goal of this thesis is to detect liveness while scanning fingerprint on an optical sensor. Even some techniques already exist, new approach will be examined in this thesis. The examined method is based on detection of change of papillary lines during several seconds of scanning. By comparing several images from video sequence the pulsation should be found.

This technique of liveness detection were previously examined by Peter Dragula in his work [1], but due to the used device and processing methods the results did not show satisfactory evidence about liveness of the finger. Therefore, one of the goals is to retrieve better results than was achieved in his work. This will be done by changing processing methods, which will be tested on his input data. Also the new capturing device will be constructed and tested.

In addition, the pulse frequency interval could be estimated to detect, whether the scanned person is calm or under pressure. Future security steps could be derived from this knowledge to protect the system or the scanned person.

The result of work would contain the comparison in measurements of correct and forge finger.

1.2 Organization of the thesis

This thesis is divided into five chapters. First chapter starts at page 3 and introduce the reader into the problem. Second starts at the page 5 and leads the reader from the basic information about biometric system (BSs) through the frauds of BSs to the liveness detection methods. In the chapter 3 (page 21) the description of used method are presented and the parameters of optical sensor are calculated. Chapter 4 on the page 35 describes the implementation tasks and presents and analyses the results. The conclusions are summarized in chapter 5 on the page 49. Then follow the bibliography, list of terms and the appendices.

2 Biometric concepts

2.1 Biometrics systems

2.1.1 Introduction

Biometrics is compound of two Greek words, *bios* (live) and *metron* (measurement). In Information Technologies (IT) biometrics means recognition of people based on their characteristic anatomical features (e.g. face, fingertip, iris, retina) or characteristic behavioral (e.g. walk, signature).

Biometric systems (BSs) use biometric to prove/recognize someone's identity by comparing its characteristic sample with other sample/s. This is used for *verification* and *identification*, respectively.

None of two samples could be the same at 100%, even through they belongs to the same person and the biometric characteristic is *constant* (not changeable in time, such as fingerprint). There are mainly two reasons for this disproportion. First, some characteristics were changed a little bit in time (e.g. face, signature) and second, conditions during the measurement are not the same (e.g. different light, humidity). Therefore the *threshold* is taken in place to determine, whether the matching score retrieved by comparison of two samples represents the same person or not. This leads to several errors, such as denying the genuine user or accepting the imposter user.

2.1.2 Model of BS

Most of the BS operates on a very similar principle and mostly consists of components shown on the Figure 2.1.

Before the process of identification or verification starts, the master template is created in the stage called *enrollment*. First, the user's identity is verified (by photo Ids, driver license, passport, etc.). Then the *capture device* acquires biometric data. Next, the *feature extraction and template construction* component processes the biometric data as a result creates the master template. The master template is referenced against an identifier (PIN, name, user ID, etc.) and is stored in the *storage* (mainly some kind of database). The whole process is controlled by *central controlling unit.*

Process during verification or identification is very similar to enrollment. However, there are differences between verification and identification. When verifying, user first presents his identity, then the biometric sample is created via the *capture device*. Next, the *current template* is created from this sample, which is compared to master template using *template matching algorithm* and matching score is retrieved. Based on *matching score* and *threshold* the *algorithm* or *central controlling unit* makes the final acceptance/rejection decision.

Process of identification is similar, however the current template is compared to all master templates in storage, because the system doesn't know the users identity at the beginning. Threshold value is set also much lower than in case of verification, because identification systems are used mainly to recognize people who wish not to be recognized. Therefore, they change their biometric characteristic and the matching score is lower.

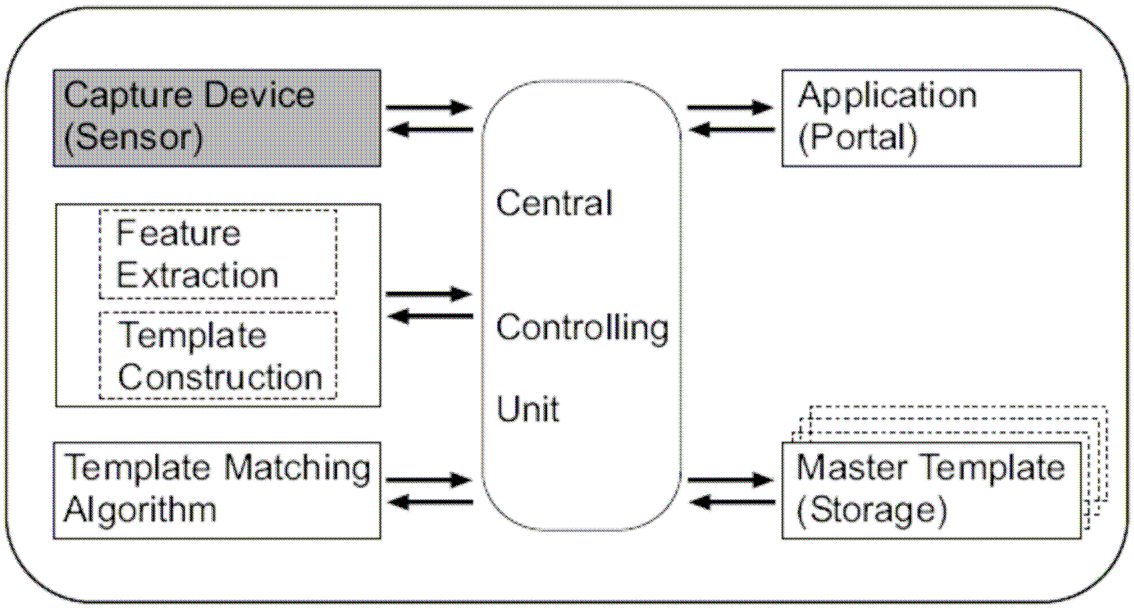

Figure 2.1. The basic model of BS [4].

2.2 Security of BS

Several possible threads to BS are known. Each component and process step of BS could be attacked. An identification of some basic threats and proposals of solutions are following:

1) **Capture device** may be fooled by being presented with a fake sample. This can be in the form of an impersonation with some incidental amount of tampering with the sensory device or process (i.e. an intruder presents a possible reproduction of a biometric feature as an input to the system). Another form is a replay attack by tampering with the sensor (i.e. an intruder has to bypass the sensor and has to resubmit the previously snooped biometric data).

   Appropriate solutions that need to be implemented to secure capturing device could be: liveness testing, tamper resistance or supervising of the system. In addition, regular inspections should not be underestimated. In the case of the protection against replied attacks, modified challenge–response protocols or data hiding are involved. Sometimes the "exact match" approach is used.

2) **Feature extraction and template construction** part could be attacked by *Trojan Horses*. Such attacks will produce a pre-selected feature set at some given time or under some specific condition. Another way to compromise the BS is to associate the identity with a poor biometric sample (i.e. “quiet” or “noisy” master template).

Possible solutions to secure this threat are: ensuring physical security (i.e. tamper resistance, guards, inspections etc.), data encryption and access control to store templates and biometric devices. Another, during the initial capture process, adding quality control of biometric characteristic helps to protect against the threat of a poor master template. On top of that, the enrollment process should include a search through existing master templates. This eliminates anybody with multi-identities property and people with very similar biometric characteristics from posing as the others.

3) **Template matching algorithm** threat is dishonest manipulation with the score to produce a very high or a very low match score, thereby affecting the final acceptance/rejection decision.

Possible solutions against this threat are: testing, verification and maintenance of the matching device and its match score. Transmitted data should be encrypted, whenever they leave a tamper-resistant or a human supervision environment.

4) **Master template (storage)** threat is unauthorized modification of one or more master templates in the database/portable device. This could lead to authorization of a fraudulent individual, or at least to denial of the person associated with the corrupted template.

Possible solutions: master templates should be stored, encrypted and digitally signed in the central database on the server to protect their integrity and confidentiality. In a case, when a portable medium is used to store the user’s master template, digital certificates are involved to ensure the template’s integrity and confidentiality. Typically, during the enrollment phase, the master template is signed by a private key of a digital certificate, which belongs to the BS. This way the integrity of the master template is assured. The private key used for such signing in the system can maintain only those parts of the BS, where the enrollment phase was executed. Next, to ensure confidentiality, the signed template is enciphered by the user’s public key and stored in a portable device. This approach is suitable, because the security of the master template is dependent upon both the user and the BS. In addition, the link between the user and his master template is created.

5) **Application (portal)** threat means tampering with the channel between the template matching algorithm and the central controlling unit and the application, which access is being required to. An intruder could also tamper directly with the application (like

a gate at the entrance to the building) to grant the access right (enter a building).

Possible solutions are the following: ensure tamper-resistance of the vulnerable parts of the system and encrypt the unsecured data.

6) **Central controlling unit** threat is based on a possibility of overriding the final acceptance/rejection decision by an attacker. As the whole process is controlled by the central controlling unit, by tampering with this part, the imposter could cause authorization of a fraudulent individual or denial of service. In addition, the *communication* threats should be included here, because the central controlling unit also manages communication between components. When the BS is under constant human supervision or its parts are maintained in a tamper-resistant box, there is no need to deal with communication threats. However, many BSs are designed to remote identification/verification purposes. In such cases, these threats have a high probability.

   Possible solutions: ensure physical security and access control to stored data and biometric devices. In addition, communication attacks could be prevented by encrypting the communication channels, supplemented with mandatory authentication of participants-ensured (e.g. by challenge–response protocols). Monitoring and auditing should not be underrated.

In this work, the fooling of BS related to the sensor (*capture device*) will be examined. A capture device might be fooled by presenting a fake sample. This could be obtained from the regular user with or without his assistance. First, the biometric characteristic is stolen by the attackers (or given, when the user is cooperating with them). Then the replica is created and presented to BS's sensor. Another type of attack related with capturing device is the association of someone identity with a false or poor quality biometric characteristic. This attack could be done during the enrollment, which could later lead to high matching score with many other templates.

Protection against these types of attacks is human supervision over the BS or liveness testing of biometric characteristic.

2.3 Fingerprints

The fingerprint is created by imprinting or scanning papillary lines of the fingertip. Papillary lines are the corrugation of top layer of skin (epidermis). They are formed in human embryonic stage and during the whole live the papillary lines drawing is unchanged (unless some physical damage is done to dermal skin layer, such as cuts). This biometric feature (characteristic) is *constant* in time.

Papillary lines are *unique* for every individual. It means that there are not two people with the same papillary texture on their fingerprints, however this has not been proven (but it also has not been

proved otherwise). Although, the one-embryo twins have a different fingerprints. Therefore, the biometric characteristic could be considered as human identity.

The fingerprint texture consists from *ridges*, *valleys* and *sweat pores.* Ridges, called also papillary lines, are a small continuous regular juts of then human skin. Valley, as the word itself says, is a hollow between two ridges. On the ridges, a lot of sweat ducts ends and forms the sweat pores. The valleys and rigdes creates the texture of the fingerprint. This is depended on papillae in dermis. Therefore, a shallow cut that affects just the epidermis, does not have effect on the texture of papillary lines after healing the wound. Just a deep cuts or scratches of dermis, which change the papillae, effects the texture of papillary lines (Figure 2.2).

Fingerprints have been used in special area of criminalistics called dactyloscopy. They helped to capture and identify criminals or victims. Later, this biometric characteristic found its usage in BS to verify people. At this time, over 50% of BS is using fingerprints [30]. The popularity is related to the several factors. The characteristic is *constant, universal* and cheap and the willingness of the users to capture fingerprints is relatively high. We said that the fingerprint has a medium *acceptance* [9].

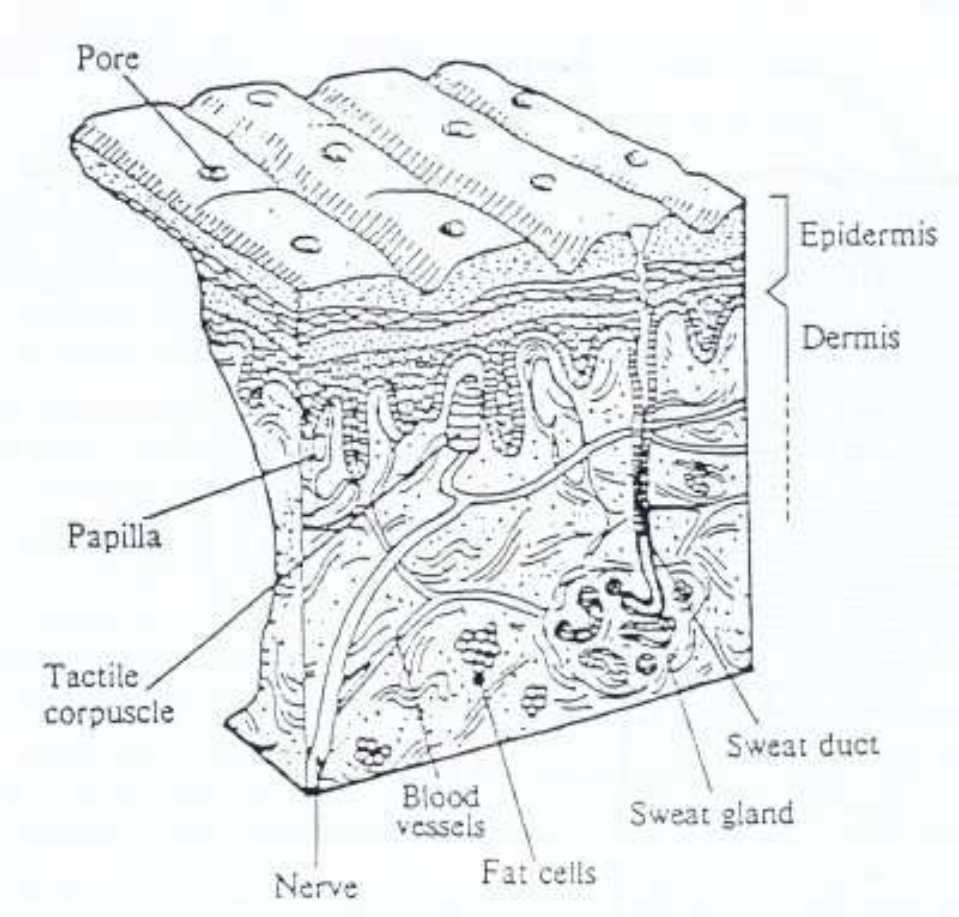

Figure 2.2. Vertical cut through skin displays papillary lines on the top of epidermis. Several sweat pore spots are also visible [12].

2.3.2 Sensors

Historically, the acquisition of fingerprint images was performed by using so-called *ink-technique*. Nowadays, there are many type of sensors, however most of them belong to one of the tree families: optical, solid-state and ultrasonic [5].

Frustrated Total Internal Reflection (FTIR) belonging to optical sensor family is the oldest fingerprint acquisition technique. The process during the capturing of the fingerprint is followed: the finger touches the top-side of glass prism, but while the ridges enter in contact with the prism surface, the valleys remain at a certain distance (see Figure 2.3); the left side of the prism is illuminated through a diffused light. The light entering the prism is reflected at the valleys, and randomly absorbed at the ridges, therefore the ridges then appears dark and valleys appears light. The light rays exit from the right side of the prism and are focused through a lens onto a CCD or CMOS image sensor. Because of different light reflection on ridges and valleys, the papillary lines could be discriminated on result image properly. According to [5], these types of sensors require three–dimensional surface to obtain image with papillary lines.

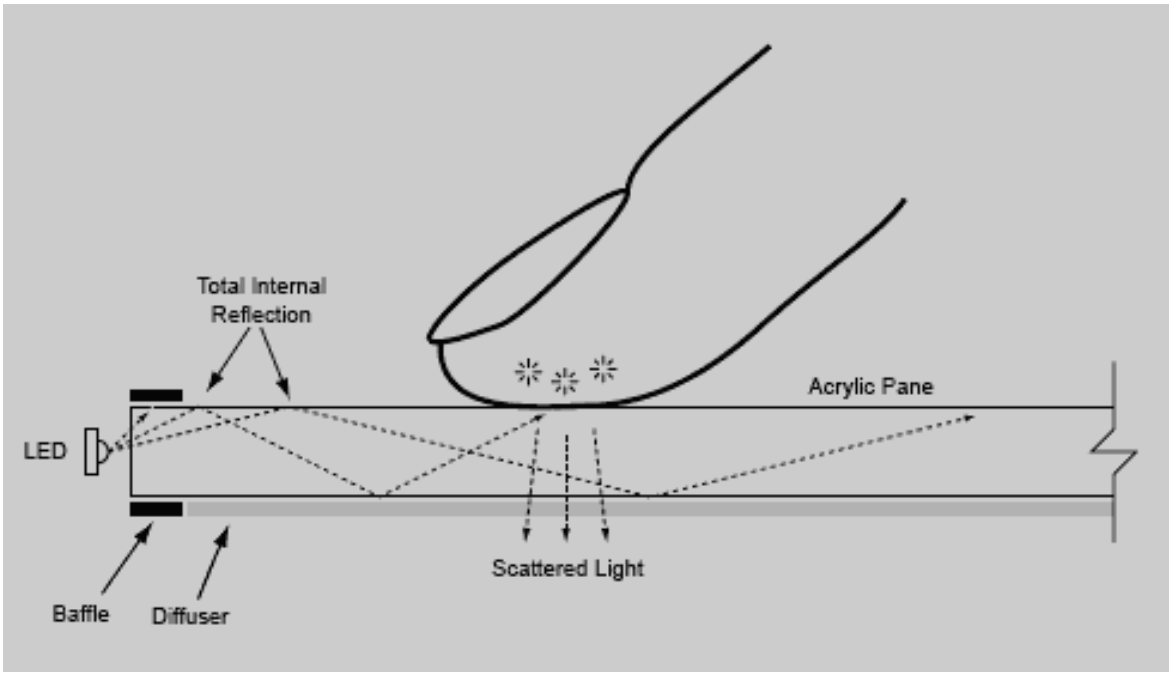

Figure 2.3. The principle of a FTIR sensor [21].

Another type of optical sensors is *electro-optical*. They consist from two layers. First is sensitive to proper voltage of the skin and emits the light. Second contains photodiode array and produce an image. Papillary lines image has light ridges (because the voltage in ridges emits the light) and dark valleys.

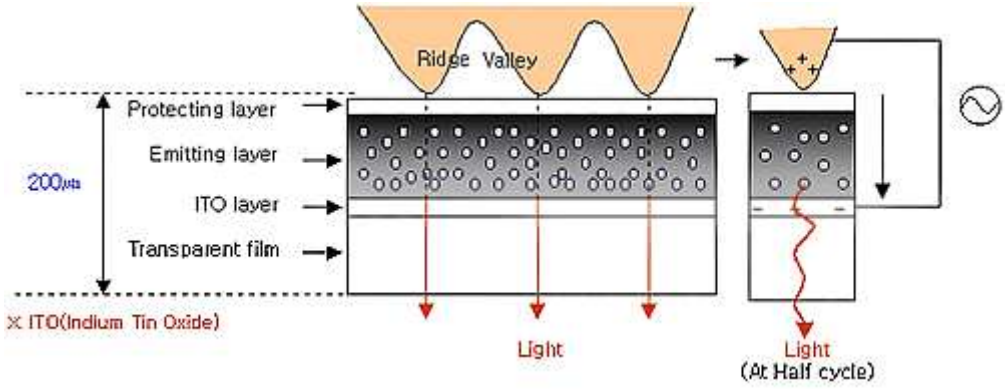

Figure 2.4. The principle and the construction of an electro-optical sensor [31].

Solid-state sensors convert the physical information into electrical signals. Four main effects have been proposed: capacitive, thermal, electric field and piezoelectric.

Capacitive sensors use the silicon-based two-dimensional sensor area with micro-capacitor plates. The principle is based on measurement of electrical charges created between two plates. Micro-capacitor plates are the first plate and the second plate is the finger itself (see Figure 2.5). The magnification of these electrical charges depends on the distance between the fingerprint surface and capacitive plates, which products different capacitive patterns on ridges and valleys. Capacitive sensors could be deceived by stamp with three-dimensional texture of a fingerprint. Even the stamp's rubber is non-electrical material; with air-humidity acts like second plate [10].

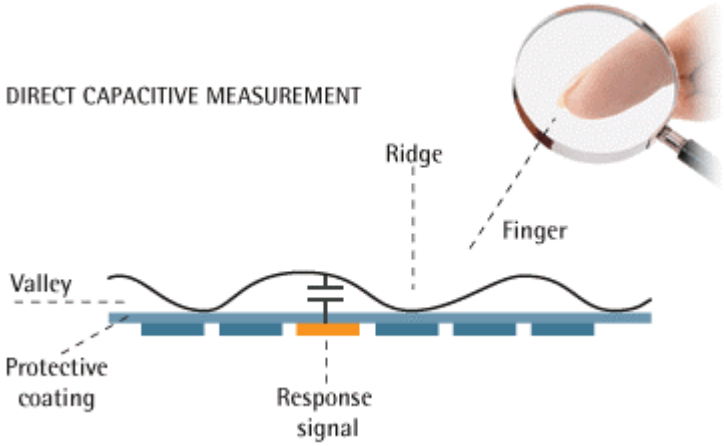

Figure 2.5. The principle of a capacitive sensor [22].

Ultrasonic sensor is kind of *echography*. It is based on sending acoustic signals toward the fingertip and capturing the echo signal. The echo is used to compute the ridge and valleys structure. This technology is resilient to dirt that may lead to low-quality image when using other type of sensor. According to [32], this technology could distinguish between real fingers and any imitations.

The initial impulse for creating the sensor was the idea of capturing (scanning) the fingerprint. Later, some new approaches were examined, either for financial or security reasons. However, not all

methods of frauds could be premeditated. Therefore, some frauds are successful against some sensors. They are described in the next section (see 2.4). On the other hand, section 2.5 presents some sophisticated methods of protection against these frauds.

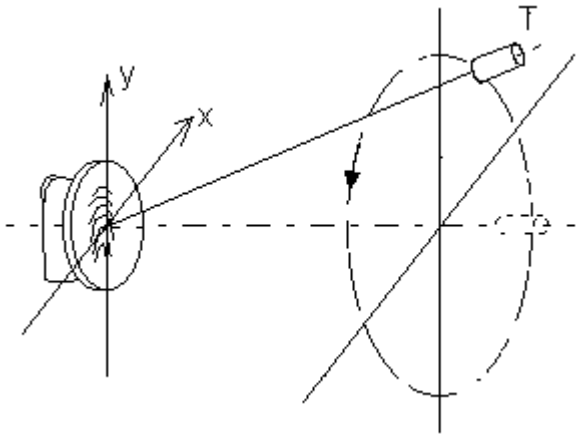

Figure 2.6. Schematic diagram of the device [32].

2.4 Frauds

To fool the sensor could be easier as anyone can even think. The simplest way is a reusing of the fingerprint that was left on the sensor (latent fingerprint). There are possibilities, how to do it:

1. **Breathing.** It is quite enough to re-activate the latent fingerprint by gentle breath. The water vapour contained in breath condenses on the surface of the sensor. Water with a combination of the grease of the latent fingerprint changes the capacitance of the surface, which is recognized as a new touch of the sensor. The sensor starts scanning "new' fingerprint, but in fact it scans the same one. This is very simple. However, sensor produces fingerprints with very low quality this way.
2. **The bag of water.** The principle of this method is same as the previous one. The only difference is that water gets to the sensor from the bag. In addition, there is more water and is placed uniformly. Therefore, the quality of obtained fingerprints is higher than gained by breathing method.
3. **Graphite dust.** Another possibility is to apply graphite dust on the latent fingerprint and than cover it with adhesive tape. After that, imposter press on the tape and the sensor accepts the fingerprint without any problem. In that, this method has 100% success. There is also a possibility of modification of this method, when the latent fingerprint is left somewhere else, e.g. on a glass (of vine in restaurant). Again, the graphite dust is applied on the latent fingerprint, tape is placed over and that pulled down. Dust that was attached to the sweat and grease on the latent fingerprint is now on the tape. Then, the tape is placed over the sensor and pressed.

These methods can be used just on those types of sensor, where the latent fingerprint could be left. It means that contactless sensors (such as ultrasonic sensors) are resistant against these types of attacks. Also compressive and electro-optical sensor could be erased from the list of non-resistance sensors, because, even if the latent fingerprint could be left on them, it cannot be reused, because these types of sensors requires three-dimensional model of finger.

Sprinkling with graphite dust might be used also with optical sensor, however, the papillary lines are displayed as white on optical sensor, but the latent fingerprint with dark dust has the papillary lines black. Therefore, the inversion of fingerprint would have to be done.

It might look like, that all types of sensors are somehow resistant. However, these methods were successfully tested on capacitive sensor.

2. **Print/Photography of the finger.** Even there is commonly known, that to fool the sensor you can just print photography of your finger, there are no researches that validate such hypothesis. Therefore, this "knowledge" is probably wrong.
3. **Stamp.** By the research of Dana Lodrova [10], to create a stamp is quite easy (there exist some stores that create any stamp you required) and you can impose with type of fake fingerprint optical, capacitive and thermal sensor.
4. **Artificial (dummy) finger.** There are two methods of creating the dummy finger: with and without cooperation of the real owner of the biometrics. When the owner cooperates with attackers, he or she wittingly allows the attackers to capture his fingerprint. Second methods assumes, that the fingerprint is left somewhere on shiny material, such as glass. Then the attackers capture the fingerprint from this surface. This is non-invasive approach. Another, invasive, and more drastic, is cutting the owner's finger (such event really happened [11]). There are several material used to create dummy finger:
    a. **Silicon.** This material was used in research of Ms Lisa Thalheim [19]. The form for the silicon was created from the wax. The form was then filled with normally available silicon. These dummy fingers were tested on optical and thermal sensors. The optical sensors from company Identix were fooled with 100 percent success. Thermal was harder to fool, but the researchers had just need to learn how to do it. Another researcher (Mr. Putte and Mr. Keunig [20]) were able to impose also capacitive sensor, just the finger had to be wet (by saliva) before the scanning.
    b. **Gelatin.** Research of these dummy fingers was done by professor Matsumoto and his colleagues [29]. He created the dummies different ways with cooperation and without cooperation with the real owner of finger. When the owner cooperated, he presses his finger in material called Freeplastic. This impression was used as a form for dummy finger.

       Without cooperation, the process was little bit complicated. First, the visibility of the latent fingerprint was increased by cyano-acryl paste. Then the photography of it was

taken. After editing in graphic editor, the latent fingerprint was printed on transparent foil. Then the foil was laid over photosensitive layer. Using UV light and followed modifications the form.

The material used for filling the form was gelatin. The advantage of this material is a bit funny. When the imposter is disclosed after using this gelatin dummy ("gummy") finger, he can eat it and destroy the evidence of imposing.

Gelatin dummy fingers were successfully tested on six optical, four capacitive and one electro-optical sensor.

c. **PlayDoh** is another possibility of creating dummy fingers. The advantage of this material is its higher humidity, therefore it can be successfully used to fool humidity-sensitive sensor. This way, the optical, electro-optical and capacitive sensors were cheated.

5. **Removed finger**. This is harder to detect, as the finger has nearly all signs of live finger (e.g. color, temperature, fingerprint texture). Just the live signs are missing (e.g. pulse, conductivity). Therefore, this "method" was successfully used to cheat capacitive, optical and electro-optical sensors.
6. **Wafer-thin fingerprint** attached to the finger (see Figure 2.7) is the most problematic and hard detectable fake technique. These wafer-thin layers are made from the same material as whole dummy fingers. They are so thin, that the liveness detection methods detect the live finger behind them.

   In addition, the human or camera supervision of the sensor has no significant effect, as this layer could be easily unnoticed by human.

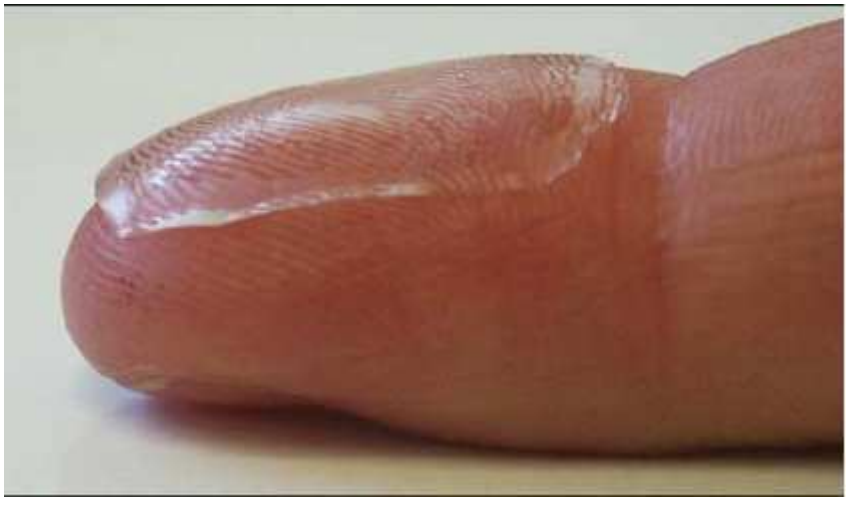

Figure 2.7. The wafer-thin dummy attached to a finger [7].

2.5 Liveness detection

To prevent against frauds during scanning, the liveness detection is being added to the sensors. Liveness detection method uses physical properties of body to detect, whether the presented finger is dummy or real. During the detection, several properties could be used at once.

Someone could obtain, that the biometric measurement itself is liveness detection. That is true in fact, however this measurement is weak, as could be seen from several successful frauds (section 2.4). The strongest biometric measurement contains also some additional biometric measurement. However, it is important, that the same part of body is measured. There is no reason to detect liveness from blinking the eye, when the fingerprint is taken. In addition, the liveness detection has to be detected during the biometric measurement. If it is not done this way, the attacker could present an artificial characteristic in step of capturing and real characteristic in step of detecting liveness. It is also important that this property is hard to simulate, or, better, could not be simulated (which is in fact not possible). At least, the property measurement has to be implementable (on the software or the hardware level) as cheap as possible.

Human body offers us many properties, which could be used for purposes of liveness detection. Just some of them are suitable for the fingerprints. These properties are described in the next section.

Liveness could be disclosed by pulse detection. In this thesis is presented a new approach of pulse detection based on changing the distances between the papillary lines.

2.5.1 Useful properties

The properties, which are useful for detecting the liveness while capturing the fingerprints on some sensor, could be divided into three main groups:

1. **Inner properties** are properties of live human body. For the fingerprint capturing could be used properties of several skin layers, fibers another body parts hidden under skin.
    a. **Physical/mechanical.** This category contains density or elasticity of the skin. The elasticity of the skin is required nearly in all types of sensors, when the person has to press the finger on the sensor. Than, in fact, thanks to elasticity, the transformation from 3D finger to 2D finger happens. By increasing the pressure on the sensor the changing of width of papillary lines could be observed. This could be used to implement a software solution based on the comparing the width of papillary lines before and after stronger pressure of the finger on the sensor.
    b. **Electrical** properties consists of the skin capacitance, impedance, resistance, conductance or dielectrically constant. These properties are used in capacitance or E-Field sensor, however, not for liveness detection, but for the capturing of the fingerprints. Human skin has different properties than other materials, which could be in liveness testing.

Conductance (or conductibility) of the skin is depended on the environmental conditions (e.g. air humidity), on the climate and character of the skin (means wet or dry fingers). As the result, the interval of acceptance values is very wide, which could be exploited.

The dielectrically constant is depended on the same conditions as conductance. The gummy fingertip wet in dilution of water and alcohol is enough to fool this type of liveness detection [10].

c. **Visual.** Here belongs the color of the skin or the transparency of the skin. There is no significance to test the color of the skin itself. At present time, an artificial finger could be easily created with the color of the skin. However, when you press the finger, it changes the color to the white. This affects the reflectivity of the skin, especially the green and blue parts of visible spectrum.

d. **Spectral.** The ability to absorb, leak or reflect electro-magnetical waves of various wavelengths comes under this category. Thanks to this, we could distinguish between many materials, which could be used for creating a dummy finger. Also the dead fibers have different abilities than the live.

   Other possibility of using this property is detection of change of light absorption during the pulsation or (similar to visual properties) light reflectance change invoked by pressing the finger.

   Also the characteristic of the reflection of the ultrasonic waves is different for live and dummy or dead finger. This change is very significant.

e. **Body liquids.** Here belongs several components of the blood, oxygen saturation of blood, DNA, etc. To process the DNA takes about half an hour. This is too long for accessing system. And, in fact, DNA itself could be used for identification, therefore capturing of the fingerprint would have no reason.

   The oxygen saturation of blood could be used for liveness testing. It requires hardware implementation based on pulse oxymeter, which is commonly used in medicine, nowadays. The functionality of this device is based on the fact, that light absorption is depended on the density liquid. The measured liquid is saturated and non-saturated hemoglobin. Also, thanks to pulsation, the amount of hemoglobin is changing.

   The oxygen saturation has also disadvantages. It is the time needed for scanning (approximately around 5 seconds – several pulse waves have to be captured) and the ability of fooling the liveness detection. This could be reached by moving the dummy finger or adding blinking light diode into to dummy finger. Also to very thin wafer-thin dummy (Figure 2.7) with fake fingerprint could impose this method

(it would be so thin, that the saturation of blood of real finger would be detected without any significant change).

2. **Generated signals.** It means the signals, which are unwittingly generated by live human being.
    a. **Pulse** (see section 3.1.1) is very important property of live human being. In fact pulse means the live. It have to be taken into consideration, that the pulse differs a lot, depending on the person, its physical and mental health, previous activity (e.g. calm walk to the sensor, or fast run). The sensors are based on pulse oxymeter (see body liquids (1.e) above).
    b. **Temperature** is not very helpful property. Normally, skin temperature on the end of finger moves between 26 and 30 degrees if Celsius. However, there are some people, that have a bad circulation of blood in the hands, so they fingers are nearly cold. Those people would be rejected by the system. On the other side, wafer-thin dummy could reach the finger temperature quite quick, so there will be no protection against this type of attack.
    c. **Sweat.** Liveness testing of fingerprints based on detecting the sweating has been already implemented. The research is lead by professor Shuchers from the laboratory BioSAL at Clarkson University and at West Virginia University [15]. This property and its usage are better described in following section (2.5.2).
3. **Stimulus reaction.** The sensor creates some kind of signal and measures the reaction in the scanned area. Reaction are divided into:
    a. **Voluntary (behavioral).** These types of reaction are influenceable by mind, which means the person is asked to do something, and then the positive reaction is measured. There is no sense to detect visual or sound signals, person have to react through the touch. Through the touch, we can distinguish temperature, shapes or roughness of the surface. However, we can not determine the temperature exactly, just relatively. So, we can say, that the sensor plate is cold or hot. There is the same problem with roughness. Either the surface is smooth or rough. And if you are not blind, your shape detection is also not so developed. So, the only possible interaction with the person, that could system provide based on this properties, are: “If the sensor plate is cold, press once, if hot, press twice.” or “If you feel some pressure in top of the finger, roll left, otherwise roll your finger right.”
    Therefore, these reactions are not helpful at all.
    b. **Involuntary (reflexive)** reactions are done spontaneously by body. We have no control over them (e.g. reaction of the iris on the light).
    At the finger, we can detect the reaction on the changing of the temperature. When the sensor heat the plate, the fingers blood-vessels expanded and more blood runs

through the finger (this could be detectable again via oxymeter). The opposite reaction comes after cooling down the plate's temperature. The advantage of this method lies in fact, that the temperature change necessary to detect the vessel reaction is so low, that human senses do not recognize it.

Another approach is the detection of the reaction on a small charge of amperage.

2.5.2 Sweat

Liveness testing research based on the detection of the skin sweating was performed at the laboratory BioSAL, led by professor Shuckers ([16], [17] and [18]). The advantage of this method (sweat detection) is clearly software solution, which means no additional hardware is required, so the existing sensors could be used. The method was successfully tested on capacitive, optical and electro-optical sensors.

Sweat comes out from sweat pores, which are on the top of the papillary lines in distance about 0,5 *mm*. Their positions are constant during the live. There are about 90 sweat pores on quadric centimeter (about 600 on quadric inch). Between the dry and wet (sweat) parts of the skin is big difference in electrical conductance and dielectrical constant, which is used to create the model of skin.

Figure 2.8. Change of fingerprints in time of capturing [10].

The method of professor Shuckers is based on the detection of a changing of the humidity (sweat) in time (see Figure 2.8). The sweat does not exist in dummy or dead (removed) fingers, therefore it could be used as a property for liveness detection for the fingerprints.

The method requires capturing the fingerprint twice, first at the moment of attaching the finger to the sensor, and second after 5 second. While the first picture is wet only around sweat pores, the second contains sweat also in part, that were before dry. It happens due to the fact that sweat spreads along the papillary lines. This can not happen with dummy or dead finger (however, I could imagine the sophisticated artificial finger that would slowly leak some salt liquid, which would simulate the sweating).

Even the description of the method look simple (the idea is simple), the implementation of the algorithm is not so easy. First, the picture has to be pre-processed to increase its quality. The median filter is used to remove the noise and then the whole image is fixed by histogram equivalence.

In the second step, the two-dimensional fingerprint is transformed on signal, which represents gray-level in input picture. This signal is calculated for both captured pictures. After that, one static and one dynamic measurement is done. The static measurement calculates the distance between sweat pores and uses Fourier transformation. The dynamic measurement compares both pictures (both signals are displayed on Tab. 2.1). The total energy of the second signal is higher than the total energy of the first one. At the first signal could be seen higher differences between the maximums and minimums.

Third step makes the acceptance/rejection decision (that means, whether the finger is live or not). For this purpose, a neural network was created and learned by several measurements. The inputs of this network are the results of static and dynamic measurements. The result is 1 when accepted, -1 when rejected.

For the testing of this method the dummy fingers was invented and created. They were made from PlayDoh and clay, which are both materials with high humidity. This was important, because the method is based on the sweating. The testing set contains 18*3 samples (1/3 live, 1/3 dummy, 1/3 dead). For the training of the neural network 2/3 of samples were used. The rest was then recognized with 100% success.

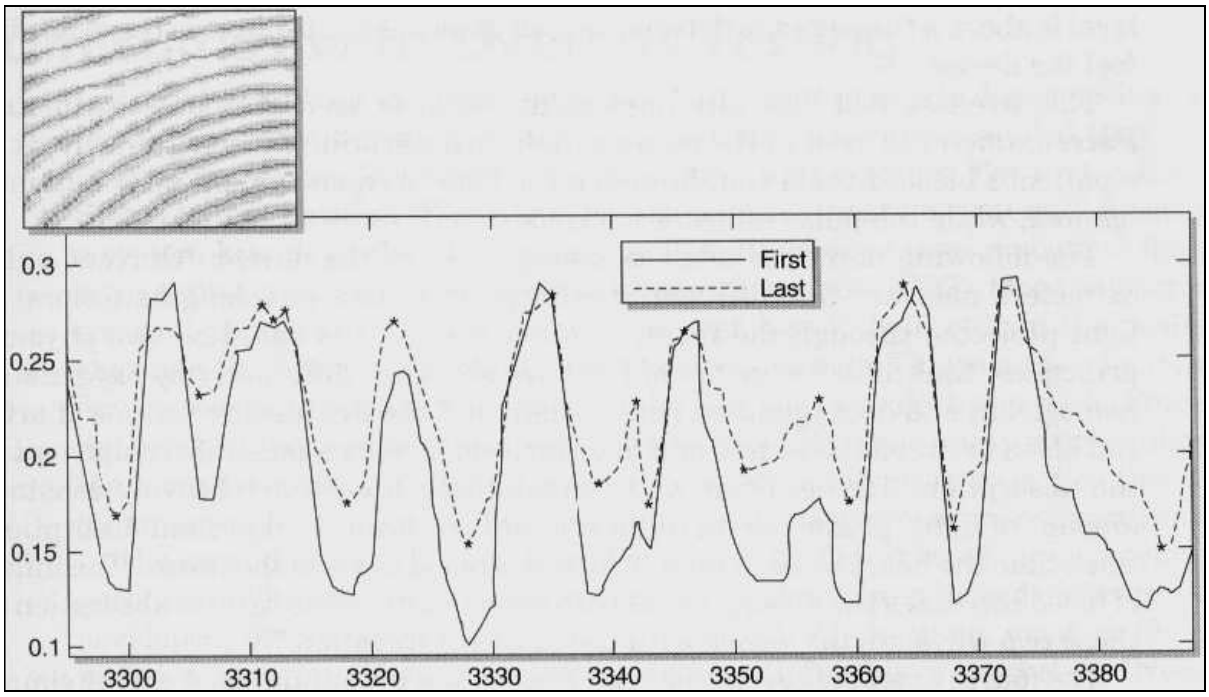

Tab. 2.1. These signals represent the amount of sweat in first and second picture. It shows the spreading and leaking of sweat [10].

Later, some other static and dynamic measurement was added, also the set of the samples were larger. However, the method haven't been tested on dependence with weather circumstances, it was tested just on the one sensor of each type (capacitive, optical, electro-optical). To fool the sensors, just the simple dummy fingers were created.

As could be seen, one task is to invent and implement method; another is to test it for several real live possibilities. My thesis consists just from inventing and implementing methods, testing these methods on input samples (my fingers and fake fingerprint printed on foil) and evaluating the results (see chapter 4).

3 Fingerprint liveness detection based on papillary lines

3.1 Used methods

Two methods of fingerprint liveness detection will be discussed and examined in this thesis. Both are based on change of papillary lines depended on the pulsation. Because the pulsation is dynamic effect, I will need sequence of fingerprint images to recognize the pulse. The parameters of sensor and camera are discussed in 3.2 and 3.3.3. The change itself is hard to capture, therefore the camera should have high resolution and the sensor should have high optical magnification. The requirements will be discussed in section 3.1.1.

First method will focus on detection of edge of papillary lines in video snapshot. It will take into concern the measurement of expandability. Such method will not be so easy to implement, because the papillary lines have to be, first of all, detected and after that the distance between neighbor flow lines is measured.

Second method will work with picture itself. The idea is following: the light absorption of finger-skin is different in *systole* and *diastole*. Therefore, we can try several image-processing methods (average gray level value, amount of pixels over some threshold value) to detect liveness.

3.1.1 Heart, heart beat, pulsation and papillary line properties

Cardiac muscle (heart) is the pump, which distributes the blood to the whole body with heartbeats. The contraction of heartbeat is called *systole*, the relaxation *diastole*. During the systole, the blood pressure is rising and a pulse wave is spreading through arteries to the body. Higher blood pressure determinates the extension of the arteries, which is measured as pulsation. Pulse wave is detectable even in capillaries in the end of fingers, which could be observed as the expandability of the skin. According to the [7], the skin on the finger expands by $13\mu m$ in diameter ($6{,}5\mu m$ in finger radius) between the systole and diastole stage.

The measurement was done on a special device by laser. The result was displayed on the diagram, where the maximal amplitude was deducted from (Figure 3.2).

According to precise measurements of the ridges and valleys distances and proportions [23], the maximal distance between two neighboring papillary lines is $0{,}7mm$. The research was trying to answer, how often the inter-papillary lines occur between papillary lines. The scientists also quantified the distances between papillary lines and the proportion (width and height) of the papillary and inter-papillary lines. All the values are displayed in the following table (Tab. 3.1).

N	Measured distance	Average value *(μm)*	Deviation *(μm)*	Minimum *(μm)*	Maximum *(μm)*
1	Inter-papillary ridge height	24,9	+/- 10,0	14,9	34,9
2	Papillary ridge height	59,0	+/- 19,2	39,8	78,2
3	Inter-papillary ridge width	194,8	+/- 65,1	129,7	259,9
4	Papillary ridge width	435,5	+/- 57,4	378,1	492,9
5	Papillary ridges distance (with inter-papillary ridge between them)	610,5	+/- 78,9	531,6	689,4
6	Papillary ridges distance (without inter-papillary ridge)	484,9	+/- 70,6	414,3	555,5

Tab. 3.1. Distances of ridges and valleys of papillary lines.

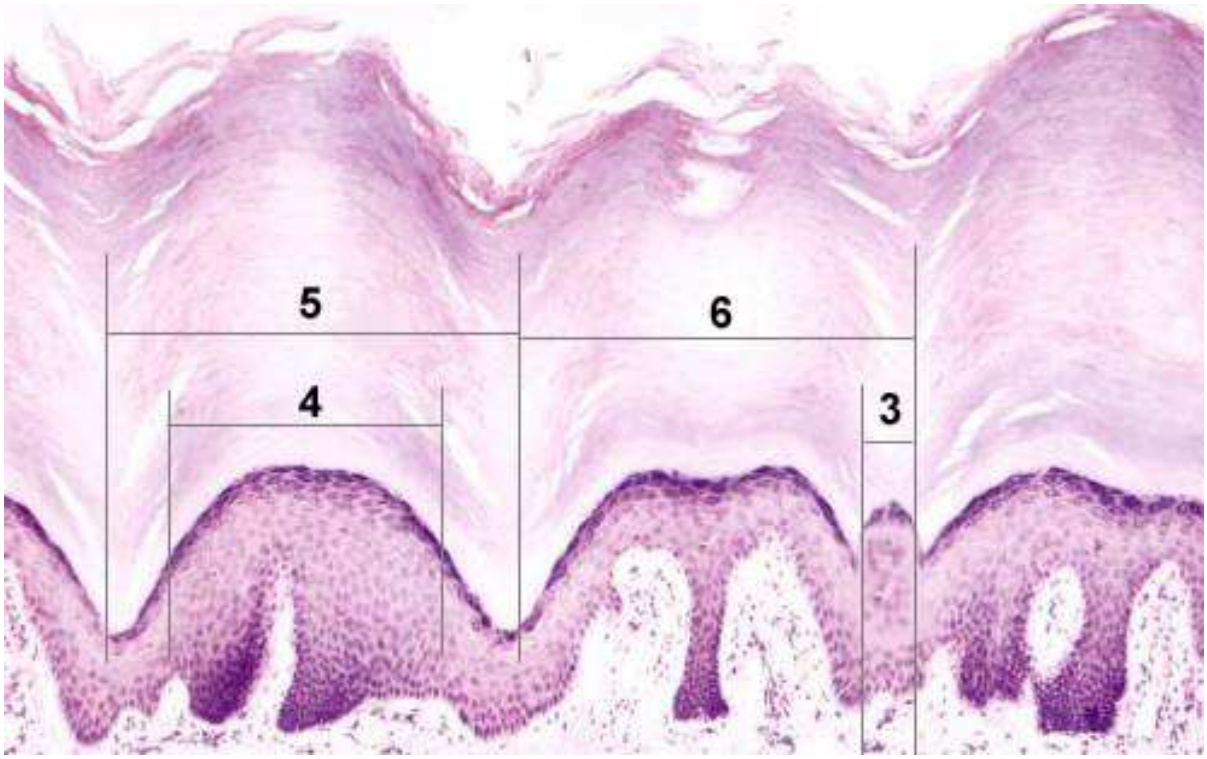

Figure 3.1. The scheme of the distances from Tab. 3.1. [33].

It is visible that the inter-papillary ridges are significantly lower than papillary ridges. Therefore, their appearance on the fingerprint image taken by optical sensor depends on the angle of illumination of the finger. With some lower value, they might be hidden in the shadow of the papillary edge.

As was written earlier, the change of width of the finger during the pulsation is very small. I would like to detect the change of the distances between the papillary lines (ridges). For this purpose, I need just a cut of fingerprint with one whole papillary line and one beginning edge of the

neighbor papillary line. As the method cannot reject someone just for his large fingers and papillary ridges distances, I have to calculate with the maximal possible value. Therefore, I assume the papillary ridges distance to be the distance between two neighbor valleys. In addition, I suppose, that the valley could contain inter-papillary line (see 6 at Figure 3.1). Therefore, I consider the distance for successful measurement to be the maximum distance between two papillary. It is 689,4$\mu m \approx 700\mu m$ = ***0,7mm***.

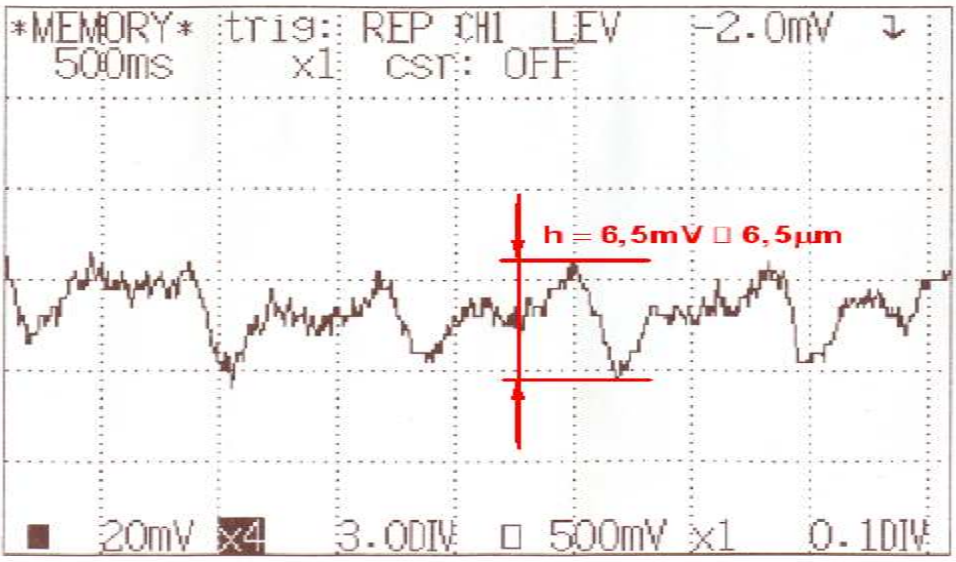

Figure 3.2. The diagram with the result of measurement of finger width in time [7].

The pulsation frequency is the amount of heartbeats per minute. A healthy human being has a pulsation frequency between 60 and 90 per minute, which rises during mental or physical stress or activity up to 120 heartbeats per minute. This number could be higher, when the person is non-trained or in a bad physical condition. It could reach 220 heartbeats per second (which in fact is the maximum, after that the heart stops and the human dies) [14].

3.2 Sensor

The sensor consists from the high definition camera with CCD or CMOS chip, and some optical macro zoom lenses. Lenses are connected to camera with standard screw thread. There are many types of threads, each manufacturer creates its own standard. These types are being used: T mouth, D mount, several Canon, Minolta or Nikon mounts for stills and C mouth, CS mouth or front-plate mount for industrial usage. These standard types allow different manufactures to connect their lenses with cameras from other manufacturer. Each type of mount defines its own *flange back length*, which is the distance between the end of lens and *back focal plane* (S_F' on Figure 3.4). Because we are looking for industrial solution, C mount and CS mount would be examined in detail.

Both C and CS mount have the same type of screw (1 inch x 32 threads per inch) and they are used for the same camera type (16*mm* movie or CCTV)[27]. They differ just in *flange back length*, which is 17,526 *mm* and 12,52 *mm* [6], respectively. There is also a possibility to connect C mount lens with CS mount camera, just the 5*mm* addition ring have to be put between lens and camera (to enlarge *flange back length* from 12,52 *mm* to 17,52 *mm*). Addition ring could also be used to increase magnification. Calculations will be explained in section 3.3.3.

Next part of the sensor is camera. As mentioned, camera should have C mount or CS mount screw thread. Widely used cameras have 1/2 inch or 1/3 inch CCD/CMOS chip. These chips have a size of cells 4,65 x 4,65 μm or 3,75 x 3,75 μm, respectively.

The detailed structure of sensor could be seen on the Figure 3.3.

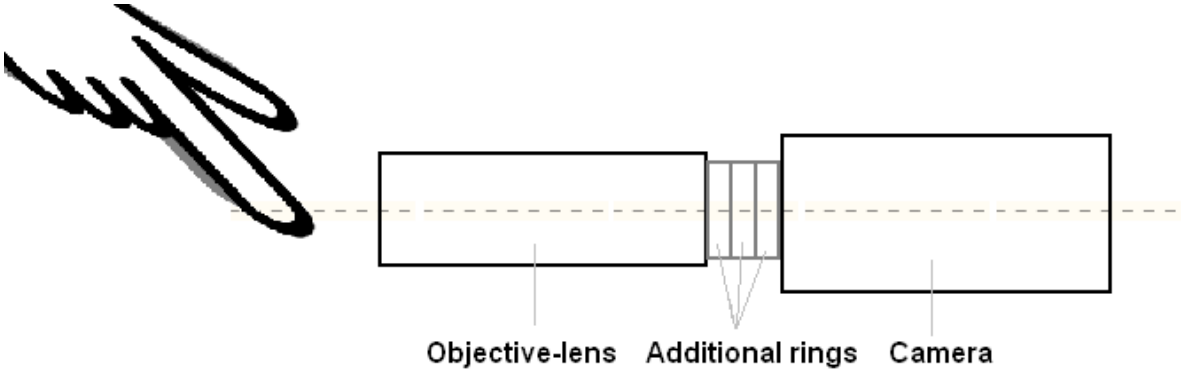

Figure 3.3. The scheme of the sensor.

3.3 Optical macro zoom lens

3.3.1 Scheme of optical lens system

Camera object lens (lens) is an *optical lens system* (compound of several lenses) (see Figure 3.4). The optical lens system captures the object (in a distance *a* from the first main plane of lens system; *y* is height of the object) and produces the image (in a distance *a'* from the second main plane of lens system; *y'* is height of the image). The front *f* and back focal length *f'* are usually not the same size. Usually, the back focal length is fixed and the front is changing as the object-lens is being focused to a different distance. The distance between front focal plane and object plane, and back focal plane and image plane is marked *z, z'* respectively.

If we take in concern one ideal thin lens, there will be just one main plane, which will be also the front and back plane of lens. However, real lens has some width. Therefore, we have to calculate with some distance between front and back lens's plane, *d*. The distance between last lens (the end of optical lens system, begging of the screw) and back focal plane is $s_{F'}$ and between first lens and front

focal plane s_F. We have to realise, that the focal length *f'* can not be measured from the end of lens system.

There is a notation, that distances belonging to object, has a minus value (-) and image distances have an apostrophe (‘).

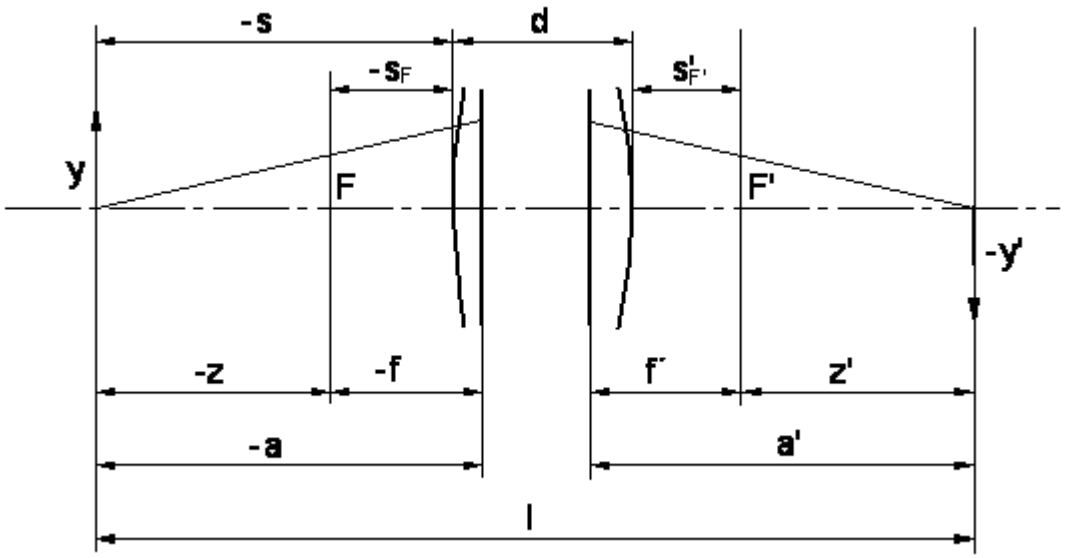

Figure 3.4. Scheme of the optical system. On the left side of the scheme is object plane; on the right side is image plane. The convention adds the minus mark to all object distances (except of the object size y).

3.3.2 Assumptions for the calculation

First, we need to realize, that the expandability of the papillary lines must be capture at least at one pixel of scanned image. Therefore, the size of change has to be evaluated. We know that the finger changes 13 μm during the pulse. Then realize that the finger is not planar. In fact, mathematically, it is some kind of deformed cylinder. If you place finger on a horizontal plate and make a virtual vertical cut, you will receive an ellipse. Ellipse could be simplified to circle. Circumference of the circle (*o*) is $2*\pi*r$, where *r* is diameter of the circle. Half of Circumference (*ho*) is then $\pi*r$. As the top of the skin expands $\Delta = 6{,}5\mu m$ (half of $13\mu m$), the circumference is expanding also. The change of circumference (cc) divided by the amount of papillary lines (*N*) gives as a change per one papillary line (*x*).

We could estimate the number of papillary lines this way. We know the sum of distance between two papillary lines and width if line itself. It is $l = 700\mu m = 0{,}7mm$. This way the estimation of number of papillary lines could be done. Next, let’s consider, that the width of the finger (no thumb) is 20*mm*, which is 10*mm* for radius *r*.

$$
\begin{aligned}
&o = 2 * \pi * r \Rightarrow \\
&ho = \pi * r \\
&ho' = \pi * (r + \Delta) \\
&cc = ho' - ho = \pi * (r + \Delta - r) = \pi * \Delta \\
&x = \frac{cc}{N} \\
&N = \frac{ho'}{l}
\end{aligned}
\tag{3.1}
$$

$$
\begin{aligned}
&r \cong 10mm = 10000\mu m \\
&d = 6{,}5\mu m \\
&l = 700\mu m
\end{aligned}
$$

$$
\begin{aligned}
&ho' = 31436{,}35\mu m \\
&cc = 20{,}42\mu m \\
&N = 44{,}78 \cong 45 \\
&x = 0.454\mu m
\end{aligned}
$$

From the previous calculation (above), I obtained the change of expansion of the skin (which happens due to the pulsation wave) per one papillary line. **The value is 0,454μm**, which is very small value. In fact, this value, that should be measured, is so small, that collides with the wavelength of visible light (0,39μm – 0,7μm). This could lead to blur problem during measurements. Another problem rises from the circle of confusion.

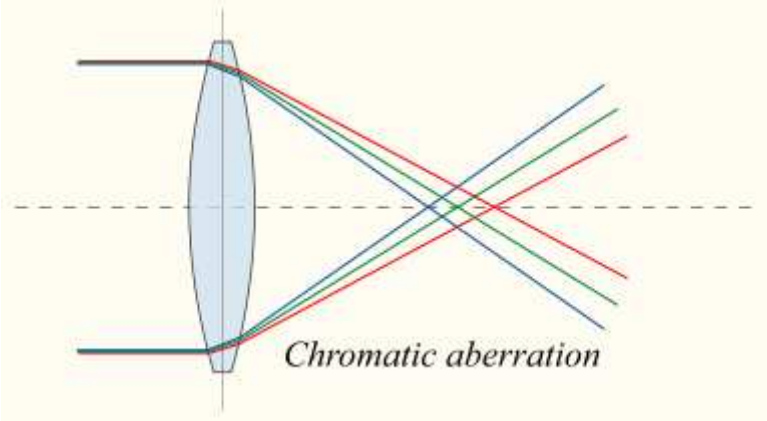

Figure 3.5. The scheme of an example of chromatic aberration [25].

None of the lenses produced precisely sharp image. When you are capturing a small point of light in infinite distance (assume very long distance) with nearly none diameter, the point displayed on the image plane will have some (even very small) diameter. This diameter is called circle of confusion (CoC) and the effect (due this happens to) is called *aberration* [13]. Usually, the CoC is being estimated as 1/1000 of focal length of the lens system, or from Zeiss formula as 1/1730 of the

diameter of the chip [24]. However, the origin of the formula itself is being questioned [24]. There also could be problem with effect called *chromatic aberration* [25]. The wavelength of the white light are in interval from 0,39μm to 0,7μm. Chromatic aberration phenomenon occurs, when the red parallel rays from object plane intersects in a different point in image plane than blue parallel rays (see Figure 3.5). The solution for this problem could be either using monochromatic light to illuminate the finger, adding photo-filter or software processing of the scanned image.

If these estimations are correct also for professional-industrial lenses, I will need either lenses with focal length about 0,45*mm* (which is nearly impossible), or camera with chip with diagonal 0,78*mm* (which is really impossible). Let's just hope that the estimations are not correct and the CoC would be small enough not to blur the result image.

3.3.3 Equations in objective-lens system

In this section, the equation used to compute several properties of object-lens system will be examined. Further, the equations will be used to calculate the values, which will be necessary to proper set up of the whole system (objective lens, camera). Nearly all formulas where taken from scripts from University of Defense [26], the rest from Wikipedia [14].

There are two main forms valid in optical system, Gaussian equation and Newton equation, respectively:

$$\frac{f'}{a'}+\frac{f}{a}=1 \tag{3.2}$$

$$m=\frac{y'}{y}=-\frac{f.a'}{f'.a} \tag{3.3}$$

where *m* is magnification (in Czech literature marked as β).

From Eq.(3.2) and Eq.(3.3) are derived:

$$f=\frac{m}{m-1}a \Rightarrow a=\frac{m-1}{m}f \tag{3.4}$$

$$a'=(1-m)f' \Rightarrow f'=\frac{a'}{1-m} \tag{3.5}$$

From Eq.(3.2), *a* and *a'* could be derived as:

$$a'=\frac{f'a}{a-f} \tag{3.6}$$

$$a=\frac{f.a'}{a'-f'} \tag{3.7}$$

Sometimes the magnification of the lens system is not enough. To increase it, addition rings are inserted between objective lens and camera. Equations for calculating the additional ring size can be derived from the Figure 3.6.

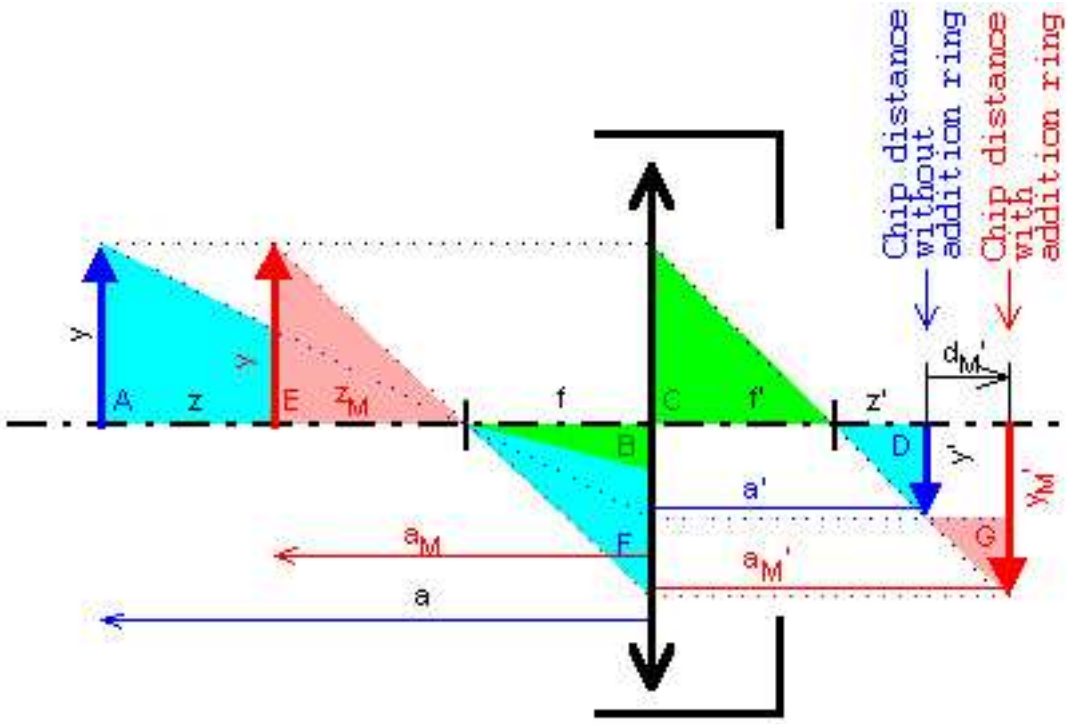

Figure 3.6. *The scheme of changing the image size and object position by adding addition ring with size of d_M'.*

First of all, the known parameters have to be marked. Let's assume, that we know the desired image size and we do not know the desired magnification and we would like to know the working position and the width of additional ring. So, we know *y, a, f', z', y_M'* and we want to calculate a_M, d_M'.

The computation starts with substituting *m* with m_M, *a* with a_M and *y'* with y_M'. The focal distances *f* and *f'* do not change. Then, the Eq.(3.2) is written as $m_M = \frac{y_M'}{y}$ and Eq.(3.5) can be written as $a_M' = (1 - m_M) f'$. Therefore

$$f' = \frac{a_M'}{(1 - m_M)} \tag{3.8}$$

Then comparing Eq.(3.5) with Eq.(3.8) we obtain:

$$f' = \frac{a_M'}{1 - m_M} = \frac{a'}{1 - m} \tag{3.9}$$

From Figure 3.6 we write $a' = f' + z'$ and $a_M' = f' + z' + d_M'$. After substituting these variables into Eq.(3.9) we obtain:

$$(f' + z')(1 - m_M) = (f' + z' + d_M')(1 - m) \tag{3.10}$$

Which is solved as:

$$d_M' = f'(-m_M + m) \tag{3.11}$$

From Eq.(3.11) we can express m_M as:

$$m_M = \frac{mf' - d_M'}{f'} \tag{3.12}$$

Using the same consecution as was used to express Eq.(3.9), we can obtain from Eq.(3.4):

$$f = \frac{m_M}{m_M - 1} a_M = \frac{m}{m-1} a \tag{3.13}$$

where the a_M is calculated from:

$$a_M = \frac{m}{m-1}.a.\frac{m_M - 1}{m_M} \tag{3.14}$$

Next, let's assume that we already have an objective-lens system. That means, we know the chip size (horizontal H, vertical V, diameter D distance and cell size), we know the parameters of the objective-lens (working distance, focal length and magnification).We know the object size, that means we also know the desired magnification m_M. We need to compute again a_M, and d_M'. To evaluate these variables could be used Eq.(3.11) and Eq. (3.14), respectively.

3.3.4 Choosing the objective lens and camera

From the previous formulas, the parameters of optic's system and objective lens will be calculated. There are many types of objective lenses. By the value of focal length, they are divided into three groups: telephoto lens, normal lens and wide-angle lens. For our purpose, first two groups are not appropriate, because both of them have a focal length to high to construct a small device. Technically, they could be used, however the sensor than will have extremely high sizes.

Another lens parameter is the magnification. Lenses, which are parameterized with this value, are industrially specialized. Therefore, the desired objective lens should be chosen either by front and back focal length values or by magnification and working distances.

To compute the focal lengths, the desired magnification has to be known. When using the 1/2'' CCD chip, one pixel has size $y_1' = -4{,}65\mu m$ (the minus is there because of notation, see Figure 3.4). Let's assume to display the expandability of papillary line $y = 0{,}454\mu m$ onto one pixel. From Eq.(3.3) $m_1 = m$ is $-10{,}24$. If we use 1/3'' CCD chip, the magnification would be different, because $y_2' = -3{,}75\mu m$. Therefore, m_2 is $-8{,}26$.

The objective lens should be chosen in depending of desired size of whole device. Let's assume, that the finger will be captured from 5 *cm* distance, $a = 50\ mm$. From Eq.(3.4) the front focal length is calculated, both for m_1 and m_2:

$$f_1 = \frac{-10{,}24}{-10{,}24 - 1} 50mm = 45{,}5mm$$

$$f_2 = \frac{-8{,}26}{-8{,}26 - 1} 50mm = 44{,}6mm$$

The back focal length also depends on “space” that the whole device provides. The working distance in the image plane is calculated from Eq.(3.5). These values are not mandatory, as the distance between objective-lens and camera could be enlarged by additional rings. It is just good to know, what will be the total length of the sensor. So, $a_1' = 9{,}24\ f'$ and $a_2' = 7{,}26\ f'$.

Therefore, either we can look for lens with focal distance around 45*mm*, or we choose from the range of magnification.

Because m_2 is smaller than m_1, the preferable chip size would be 1/3’’. However, the influence of thermal noise (and other types of noises) decreases with chip size. Therefore, 1/2’’ chip would be better due to image quality.

At last, the video capturing speed has to be calculated. Let’s assume, that human could have maximum 220 heart beats (pulses) per minute ([10]), which is nearly four beats per second. Each pulse should be quantified at least by three images, to avoid capturing images only in time between systole and diastole. That could lead to sequence of images without any significant change of papillary lines. Therefore, the chip with the ability to capture at least 12 frames per second is necessary.

3.4 Available sensor

Our laboratory sensor (Figure 3.7) consists from Computar MLH-10X Macro Zoom Lens [8] and industrial camera Sony XCD-SX910CR [34].

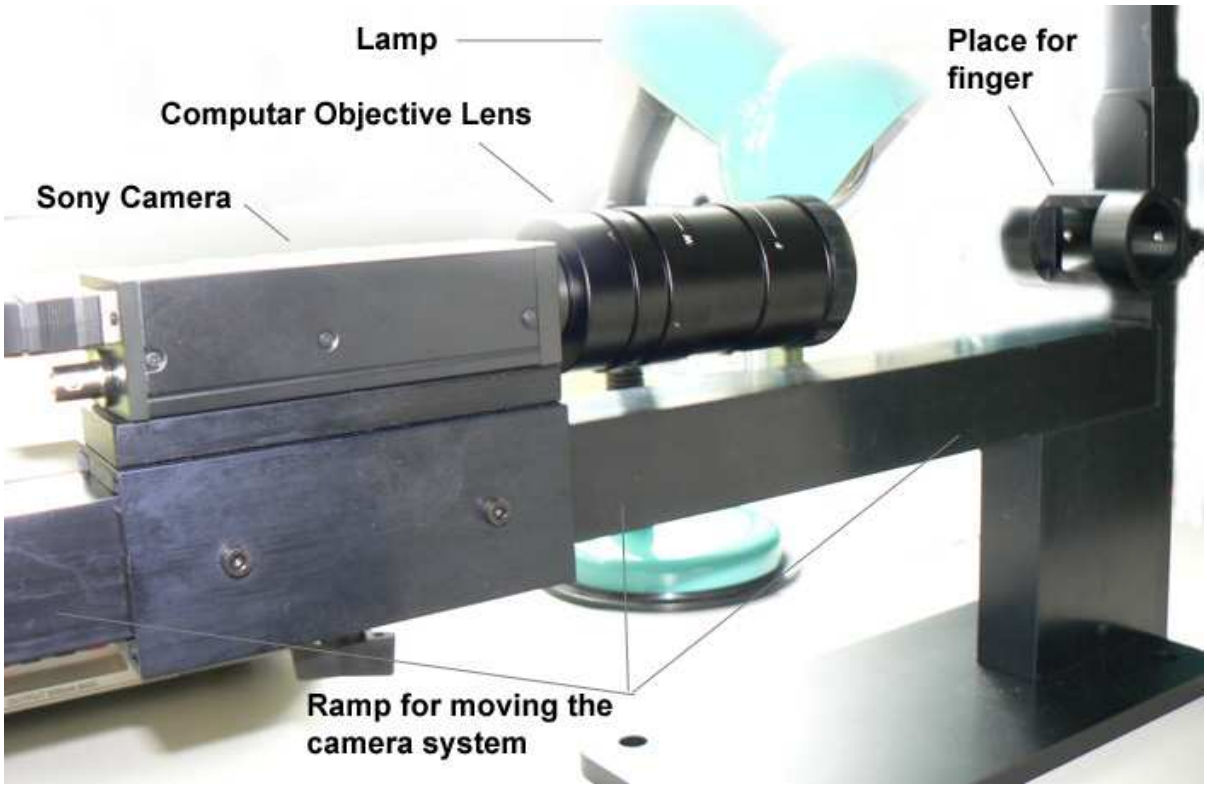

Figure 3.7. Our laboratory sensor.

Computar Zoom Lens has a minimal working distance of this lens $a = 152{,}4mm$. At this distance, the magnification is between 0.084 (wide) and 0.84 (tele) [28]. The back focal length is $f' = 23{,}29mm$, that means the finger will be placed in distance $15cm$ in front of the lens and the image is created $2{,}3cm$ behind image primary plane. The real distance from the back of the objective is called *flange back length* and is not the same as back focal length. The lens has a standard type of mounting camera, the C-mount. Therefore, *flange back length* for this type of mounting is $17{,}526mm$.

Sony camera does not have the desired parameters. Although it is able to capture 15 frames per second in this resolution and the output is 256-grayscale monochromatic image, the frame resolution is just 1280 (H) x 960 (V) (even there is high definition 1/2'' CCD chip with resolution 1392 x 1040). As we need to capture the change ($0{,}454\mu m$) at least at one pixel and we need to capture two papillary lines on the image (distance between two papillary lines was estimated as $0{,}7mm = 700\ \mu m$), we need 700/0,454 = 1541 pixels. Because we do not know the orientation of papillary lines in advance, this value should be the smaller one, which means vertical.

3.4.2 Set up the sensor

As was calculated previously, the desired magnification is $m_M = -10{,}24$. The lens itself can set up the magnification only to -0,84. Therefore, some additional ring is needed. To compute its length, I use the Eq.(3.11):

$$\begin{aligned} d_M' &= f'(-m_M + m) \\ &= 23{,}29(10{,}24 - 0{,}84) \\ &= 218{,}926mm \\ &\cong 219mm \end{aligned}$$

Calculated ring size is about $219mm$, however the lens has just $5mm$ ring included (because the screw are the same for C and CS camera, we can use reduction ring as additional ring). Let's calculate what magnification we can get from using this $5mm$ ring. To this purpose we will modify the Eq.(3.11):

$$\begin{aligned} m_M &= \frac{d_M' - f'm}{-f'} \\ &= \frac{f'm - d_M'}{f'} \\ &= \frac{23{,}29 * (-0{,}84) - 5}{23{,}29} \\ &\cong -1{,}055 \end{aligned}$$

Now, new working length, the distance between lens and finger, has to be calculated. We use the equation (3.13):

$$\begin{aligned} a_M &= \frac{m}{m-1}.a.\frac{m_M - 1}{m_M} \\ &= \frac{-0{,}84}{-0{,}84-1}.(-152{,}4).\frac{-1{,}055-1}{-1{,}055} \\ &= -135{,}52mm \\ &\cong 136mm \end{aligned}$$

At least, just calculate how much μm we can scan at one pixel at this magnification (Eq.(3.3)):

$$m = \frac{y'}{y} \Rightarrow y = \frac{y'}{m} = \frac{-4{,}65}{-1{,}055} = 4{,}4\mu m$$

No.	Description	y (μm)	y_M (μm)	y' (μm)	y_M' (μm)	m	m_M
1	**Without ring**	**5,535714**	**5,535714**	-4,65	-4,65	-0,84	-0,84
2	**1*2x ring**	**2,767857**	**2,767857**	-4,65	-4,65	-1,68	-1,68
3	**2*2x rings**	**1,383929**	**1,383929**	-4,65	-4,65	-3,36	-3,36
4	**3*2x rings**	**0,691964**	**0,691964**	-4,65	-4,65	-6,72	-6,72
5	**4*2x rings**	**0,345982**	**0,345982**	-4,65	-4,65	-13,44	-13,44
6	**Only d_M'**	**5,535714**	0,454	-4,65	**-56,6857**	-0,84	-10,24
7	**1*2x + d_M' rings**	**2,767857**	0,454	-4,65	**-28,3429**	-1,68	-10,24
8	**2*2x + d_M' rings**	**1,383929**	0,454	-4,65	**-14,1714**	-3,36	-10,24
9	**3*2x + d_M' rings**	**0,691964**	0,454	-4,65	**-7,08571**	-6,72	-10,24
10	**4*2x + d_M' rings**	**0,345982**	0,454	-4,65	**-3,54286**	-13,44	-10,24
11	**3*2x + 5mm rings**	**0,691964**	**0,670542**	-4,65	**-4,79855**	-6,72	-6,93468
12	**5mm + 3*2x rings**	**0,551115**	**0,551115**	-4,65	**-**4,65	-8,43744	-8,43744

Tab. 3.2. Several possible settings (attached rings) of the capturing device. The real and desired high of the object and magnification is displayed.

No.	a (*mm*)	a_M (*mm*)	f'(*mm*)	d_M'(*mm*)	H(px)	H(µm)	V(px)	V(µm)
1	152,6	**152,6**	23,29	0	1280/**169**	**7085/**933	960/**127**	**5315/**700
2	152,6	**152,6**	23,29	0	1280/**338**	**3542/**933	960/**253**	**2658/**700
3	152,6	**152,6**	23,29	0	1280/**675**	**1771/**933	960/**506**	**1329/**700
4	152,6	**152,6**	23,29	0	1280/**1349**	**885/**933	960/**1012**	**665/**700
5	152,6	**152,6**	23,29	0	1280/**2698**	**442/**933	960/**2024**	**333/**700
6	152,6	**76,46846**	23,29	**218,926**	1280/**2056**	**581/**933	960/**1542**	**436/**700
7	152,6	**105,0015**	23,29	**199,3624**	1280/**2056**	**581/**933	960/**1542**	**436/**700
8	152,6	**129,0844**	23,29	**160,2352**	1280/**2056**	**581/**933	960/**1542**	**436/**700
9	152,6	**145,8051**	23,29	**81,9808**	1280/**2056**	**581/**933	960/**1542**	**436/**700
10	152,6	**155,9025**	23,29	**-74,528**	1280/**2056**	**581/**933	960/**1542**	**436/**700
11	152,6	**151,9881**	23,29	5	1280/**1392**	**858/**933	960/**1044**	**644/**700
12	135,7	**135,7**	23,29	0	1280/**1694**	**705/**933	960/**1271**	**530/**700

Tab. 3.3. Several possible settings (attached rings) of the capturing device. The working distances, focal distance, ring size and chip parameters are shown.

At this point is clear, that the small 5mm additional ring is useless without some other adjustments. So, two rings, each with magnification factor 2x are used. If only the multiplicative rings

are used, the working distance is not changing. Therefore, when one ring will be used, the magnification is 2*(-0,84)=-1,68. If two will be used, the magnification is 2*2*(-0,84)=-3,32. There is also a possibility of a combination of multiplication rings and 5*mm* ring. The results are shown in table above (Tab. 3.2 and Tab. 3.3). Values formatted as bold are calculated from the other values in the row.

Tab. 3.2 and Tab. 3.3 desire an explanation. First of all, it is one big table divided into two, because there was not enough space to place all values into one table. Follows the description of the columns of Tab. 3.2:

- **description** tells us, how many and what type of rings were attached.
- ***y*** is the high of object displayed on one pixel of the chip without attaching $\boldsymbol{d_M'}$ additional ring behind the lens or last 2x ring.
- $\boldsymbol{y_M}$ if the value is not formatted bold, it is desired value of high of the object; otherwise, when the displayed value is formatted bold, it is the object high after attaching $\boldsymbol{d_M'}$ additional ring.
- ***y'*** is constant and represents the size of chip cell (that means the high of image).
- $\boldsymbol{y_M'}$ tells us, how high is the image of *y*, when the magnification of the optical system is $\boldsymbol{m_M}$.
- ***m*** represents the magnification of lenses (when none ring is attached, it is -0,84; when one 2x ring, it is -1,68; when 5*mm* ring is attached before three 2x ring, it is -8,4; etc.).
- $\boldsymbol{m_M}$ stands for a magnification after attaching the additional ring of size $\boldsymbol{d_M'}$. This value is either calculated from $\boldsymbol{d_M'}$, or is set and then effect the $\boldsymbol{d_M'}$.

On the Tab. 3.3 the result of magnifications are displayed. Description of the columns is following:

- ***a*** has a constant value, that represents the working distance without additional ring (2x rings are not mend to be additional rings here).
- $\boldsymbol{a_M}$ is a working distance, that should be set, when additional rings (with total size of d_M' – 5th column) will be attached between lens and camera.
- ***f'*** represents the focal distance in image plane, that should not change
- $\boldsymbol{d_M'}$ is the total size of addition rings, that are attached between lens and camera to achieve magnification $\boldsymbol{m_M}$. The other values in the table are depended on this value.
- ***H(px)*** represents the couples of value, which are depended on ***H(mm)*** and $\boldsymbol{y_M}$. First value is the horizontal size of a chip of Sony camera. The second is the amount of pixels in horizontal direction, which are used to display 933μm.
- ***H(mm)*** represents the couples of value, which are depended on H(px) ***)*** and $\boldsymbol{y_M}$. First value is the horizontal size of the whole object, which is displayed at 1280px.

The second is the minimal size in micrometers for capturing the distance between two papillary lines on one image (horizontal to vertical is 4:3, the distance 700μm in vertical direction means 933μm in horizontal direction).

- ***V(px), V(mm)*** the same as ***H(px)*** and ***H(mm)***, just for vertical direction

Let's explain the numbers in the table-rows. First five rows (1-5) are using just 2x multiplication rings (or none). The sizes of additional rings are set to 0 (the size of the multiplication ring should not be taken into consideration). Therefore, the magnifications and object sizes are the same. The interesting values are in last four columns, which describe the chip sizes. For example, from the first row we see, that when we use the chip with resolution 1280x960, the object has a size of 7,085x5,315mm. So, one papillary line of size 700μm (which is also the distance between two neighbor papillary lines) is displayed on 127 pixels.

Next five rows (6-10) calculate with some additional rings attached. This value is however calculated from the desired magnification and object size, which is -10,24x and 0,454μm, respectively. That means that the size of 0,454μm is displayed on one pixel. However, the amount of pixels is not high enough to capture whole width of papillary line (the object size is just 581x436μm). To capture whole 933x700μm the chip with resolution of 2056x1542 pixels is necessary. In the row 10, the additional ring size has a negative value. This means, that the magnification obtained by attaching four 2x multiplication rings is higher than necessary.

Next two rows (11 and 12) stand separately. First one displays the parameters of device, when 5mm additional ring is used after three 2x multiplication rings. The second setting places the 5mm ring before three multiplication rings. Therefore the ***a*** and ***m*** have a different values.

The conclusion from these tables is following. The best settings for purpose of this work is the setting 4, because the result object size, when using existing laboratory camera (with chip of resolution 1280x960) is nearly as big as desired. Object size displayed on the chip is 885x665μm and the desired is just a little bit higher, 933x700μm. For the experimental input data this should be enough.

4 Implementation and results

In this chapter, the choosing of implementation language is discussed, the implementation tasks and solution is examined and at least the result is presented. The comparison with previous work (done by Peter Dragula in 2007) is examined.

4.1 Requirements

Mainly, the implementation task consists from image processing. For this purpose, the best solution is to use some MATLAB, because it allows easy work with multimedia data. Also we do not need any GUI, as the result could be presented as a chart (diagram).

4.2 Input data

Because this work follows the work by Peter Dragula, with a goal of reaching better results, first his testing data are being used. An image from his sequence is shown on Figure 4.1. His sequence has 37 images with resolution 740x287 pixels. The data were taken from the different device than is described in this thesis in section 3.2.

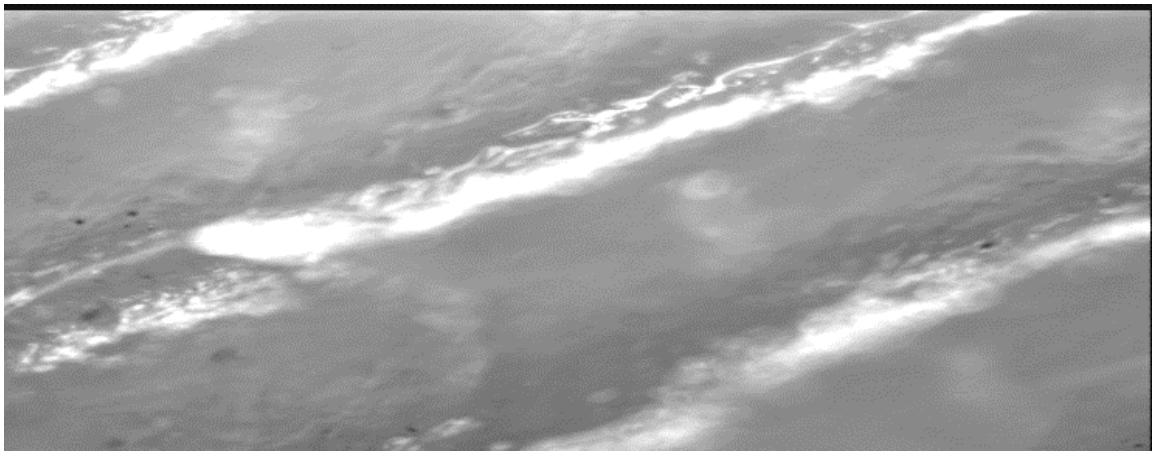

Figure 4.1. Example from sequenced of images used by Peter Dragula. There are three papillary lines [1]. The dark borders are a part of the input data.

Then I made my sequences of pictures. First, I made a several sequences with printed fingerprint, to find out, how the device will be précised and to determine the size of noise in the signal. The printed image was still and stable, however I simulate some effects of environment and possible frauds by vibrating the table and eclipsing the source of light. Then I made several sequences on a live finger.

I have to used the settings 1 from Tab. 3.2, where the magnification is just 0,84x. The reason, why the recommended settings 4 can not be used is simple. The delivery from the manufacturer of multiplication rings is delayed.

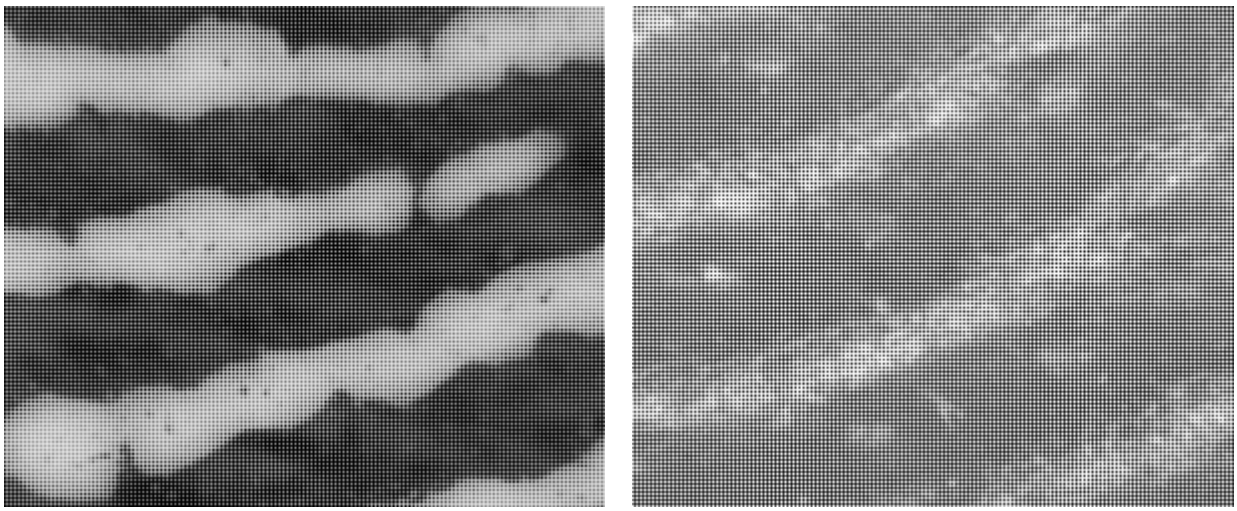

Figure 4.2. The example from my sequences. On the left, cut of the printed fingerprint image, and on the right, cut from the image of live finger.

The sequences of pictures required some preprocessing. First sets were captured as GBR24 RAW image format, where each part of the color (G,B,R) requires one pixel in output image. Therefore the resolution of the images were reduced both in horizontal and vertical dimension by two. Next sets have maximal possible resolution and set the output format to Y800 RAW, where one color channel is missing. This is not a big problem, because the light reflected from the finger is mainly around red spectrum of the colors. In fact, the green and blue parts of the white light are paucity presented. Then, for some measurements, the images were cut, so just two or three papillary lines were on them. Full resolution of the images contains about 15 papillary lines. This happens because the settings 1 from Tab. 3.2 were used. Additionally, the sequences of the fake fingerprint should be inverted (white to black and vice versa), because on the printed image the edges were black, however on the live they are white. This was done to test the algorithm and the methods, not to fool the liveness detection.

4.3 Implementation tasks

The input data is a set of sequenced pictures in TIF or BMP format. Pictures are gray-scaled with 256 colors. Whole set could be loaded to the field by one command. First of all, images have to overlay themselves that way, which the papillary lines of one image are above papillary lines of another's images and valley overlays the valleys. For this step, a sweat pore is very helpful, because it is the darkest place on the image. However, just one should be presented at each one.

At this point, sequence of images is pre-prepared for several methods of liveness detection. Each will produce a diagram, where the values will be displayed. Each image from the sequence is represented by one value. The value could be:

1) **Average gray value in image**

   Because the amount of light reflected by the skin is changing during the pulsation, brighter and darker images should uniformly switch in the sequence. Even the difference between the brighter and darker images can not be seen by eye, it could be determine as a difference between average gray values in following images.

2) **Sum of values of the image after threshold**

   Threshold image contains only two values: 0 represents the valleys and 1 represents to papillary lines (ridges). Again, the principle of changing light reflection is used. However, now the ones are counted (sum of all values). This value is calculated for each image, the higher difference between two following images in the sequence could represent the pulsation.

3) **Average width of the papillary line.**

   The expandability of the skin during the pulsation is taken place also in this method, just now the changes of width of one papillary line is measured. Again, for each image as much as possible measurement is done and then the average value is computed.

4) **Average distance between two neighbor papillary lines.**

   As the skin is expanding during the pulsation, the papillary lines changing their relative distance. Because the image of papillary lines is quantified to pixels and threshold, the distance should not be calculated just from one measurement. Therefore, as much as possible measurements are taken and then the average value is calculated.

5) **One width of the papillary line**

   Same as 3, but just one width of each image of the sequence is obtained. This method cannot adapt to slight movement of finger during scanning. It is used only to calculate the amount of noise in image sequence during capturing the printed fingerprint.

6) **One distance between two neighbor papillary lines**

   Same as 4, but just one width is obtained, not the average value of all them. This method cannot adapt to slight movement of finger during scanning. It is used only to calculate the amount of noise in image sequence during capturing the printed fingerprint.

4.3.1 Adaptive threshold

One of the implementation tasks was the threshold of the image. When I was processing Peter Dragula's data, at the beginning I used fixed value. However, later I found out that this approach does not lead to good results. Therefore, I implement the adaptive threshold.

Normally, adaptive threshold is being set for whole image. For better results, I decided to go further and I divided the image into several unique-sized areas. Then, for each one I set the adaptive threshold separately. To set up the threshold value, a histogram was created (histogram is a grayscale function, which represents the amount of each grayscale in the image). When the histogram values were calculated, they were smooth by floating window to suppress local extremes. The adaptive threshold was set from the smoothed histogram. Because the papillary lines were represented by values in upper quarter of grayscale (190..255), the threshold is set at the place of minimum of the histogram function after the value 190. When the image is threshold, there are just two values presented (0 and 1).

It is ridiculous, but the best threshold for my sequences is a fixed value, which is a little about the average gray value of the image. The reason, why my data does not need so time consuming method as the adaptive threshold (over gridded image), is quite simple. I used different angle in incoming rays. Peter Dragula used direct light from the top. However, I used front-top-left direction. Simple table lamp was used to illuminate the finger. I think that slightly better results could be achieved by using narrower beam of light, such as LED diode.

Later, another method to threshold the image was used. I called it adaptive fixed threshold. As adaptive threshold, I divide the image into several unique-sized areas. Inside each of this area I set the threshold separately. First I calculate the average gray value inside the area. Then I set the threshold value to be greater by 20 than the average value. This method is useful mainly for those images, which shades to the dark from the center to the border of the image.

4.3.2 The distance between two papillary lines

Another, more complicated task was the calculation of distance between two papillary lines. The main problem is that the papillary lines could be oriented by any angle in the image. Someone could says, that the rotation would be good idea. However, with the rotation of the image comes the loss of the information. Therefore, it is better to calculate the orientation (direction of the papillary line) and then calculate the normal. A normal is the direction of shortest distance to another papillary line.

The calculation of the orientation was pretty hard stuff. Several possibilities were examined, and at the end, as a best solution, the following process was chosen:

1) The image is divided into squares of size 8x8 (this size was set during testing)
2) Those squares, which contain at least 25% of some papillary line and maximum 75% of some papillary lines, are used for further processing. Another description could be: those squares, which average value is between 0,25 and 0,75.
3) The orientation in chosen squares is calculated.
4) Average value of orientation is calculated from the chosen squares.

The relation between the normal (n) and orientation (k) is $k = -\frac{1}{n}$. The average distance between papillary lines is then calculated this way:

1) Several lines are created in direction of normal. The interval of starting points of the lines is set on axis x(it is depended on the normal value). Let's mark it as sx.
2) For each sx is create a virtual line, that goes through points [x; n*x]. Then two situations may happen:
    a. If [sx; n] is 0, then the line starts in valley and the distance is calculated as the distance between two entering edges (a place, where [x+1; n*(x+1)] – [x; n*x] = 1)
    b. If [sx; n] is 0, then the line starts in valley and the distance is calculated as the distance between two leaving edges (a place, where [x+1; n*(x+1)] – [x; n*x] = -1)
3) The distances of lines are averaged.

During this process also the average width of papillary lines are calculated, because each line at least one cross whole papillary line.

4.4 Results

4.4.1 Sequence by Peter Dragula

From all of my methods I obtain better results than were achieved by Peter Dragula. His result is shown on the Figure 4.3.

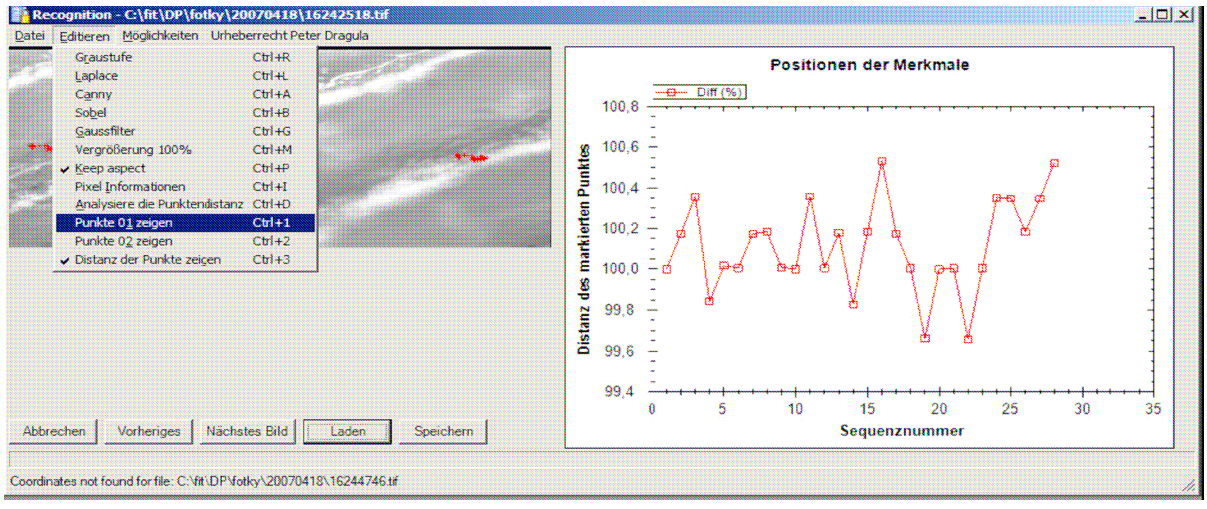

Figure 4.3. Results by Peter Dragula (the diagram on the right side of the image) [1].

My results are shown on the following images (Figure 4.4, Figure 4.5, Figure 4.6, Figure 4.7). First one displays the average gray value in the sequence of images, second the sum of values of the

image after threshold, third the average distance between two papillary lines and fourth one the average width of one papillary line.

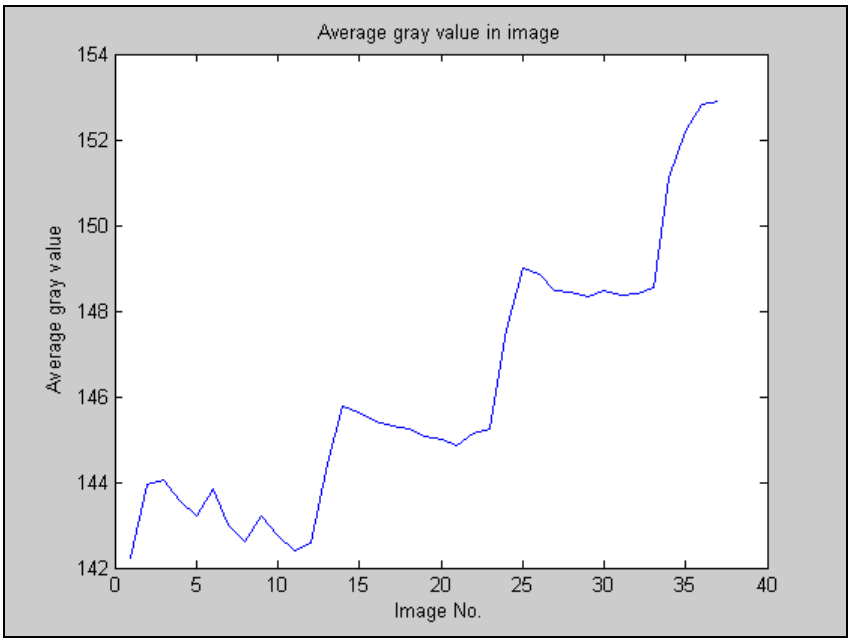

Figure 4.4. Average gray value in the sequence of images.

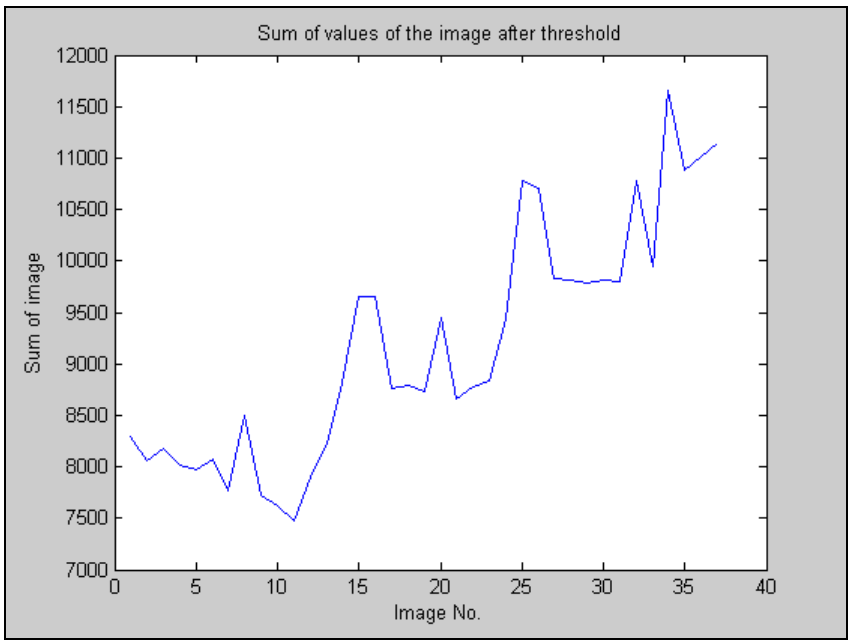

Figure 4.5. The sum of the image after the threshold.

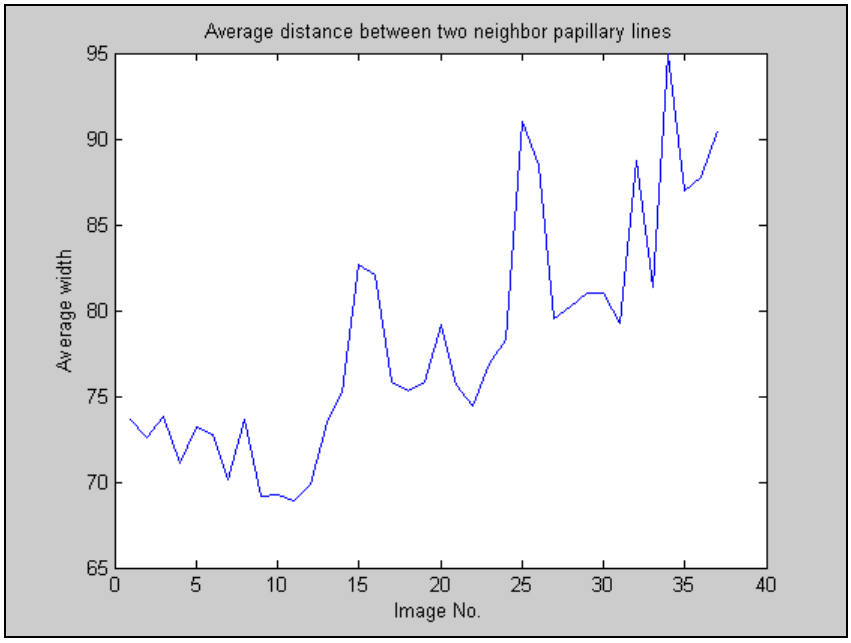

Figure 4.6. The average distance between two neighbor papillary lines.

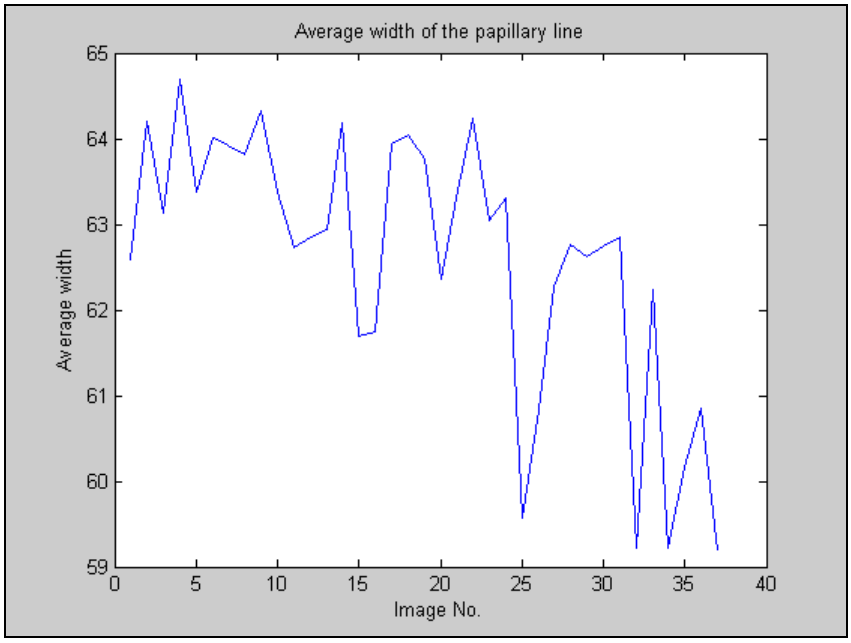

Figure 4.7. The average width of the papillary line.

4.4.2 Conclusions from Dragula's sequence

From all the images could be seen, that some significant change occurs at 15th and 25th picture of the sequence. Similar change, however not so significant, could be seen on Peter Dragula's results. As the distance between changes is 10 pictures, they should occur also on the 5th and 35th picture. In fact, all diagrams except of Figure 4.7 shows there some insignificant change.

Let's assume that the change represents the pulsation. Unfortunately, I do not know the capturing frame-rate of the sequence. Therefore, I cannot estimate the hearth-beat frequency.

However, from the average frequency, which is about 80 hearth-beats per minute (HBpM), could be estimated the approximately capturing frame-rate. So, 80HBpM multiplied by 10images gives 800 images per minute, which is 13,3 images per second. This could be, depending on the camera properties, 12,5 or 15 frames per second.

One other interesting knowledge could be deducted from the Figure 4.7. The width of papillary line is not expanding at the pulsation, but truncating. Let's estimate the change in μm.

Peter Dragula estimates 1px of the image of his sequence to $5\mu m$. Let's focus on the images 22 and 25 on the Figure 4.7. The width of papillary line is about 64pixels at image 22 and 60 pixels at image 25 of the sequence, which is $320\mu m$ and $300\mu m$, respectively. This is out of tolerance $435{,}5 \pm 57{,}4\mu m$ (given by Tab. 3.1). This could be done, however, by threshold of the image or by illumination of the finger. Therefore, the width of papillary line calculated from picture is narrower than proposed by Tab. 3.1. The contractility of papillary line is about $20\mu m$.

To test, if the diagram displays the correct distance, I have to use the Figure 4.6. The distance is calculated between two entering or two leaving edges of papillary lines. The threshold or illumination has the same influence on both edges, so it should not affect the distance between them. On the image 22, the distance is about 75pixels, which is $375\mu m$. On the image 25, the distance is about 90 pixels, which is $450\mu m$. The expandability calculated from these values is $75\mu m$. The distances between two papillary lines are somewhere around minimal allowed value from the Tab. 3.1 ($414\mu m$).

The expandability between two papillary lines was calculated from the equations to be about $0{,}7\mu m$. On the other hand, from the sequence of images it is about $75\mu m$. Therefore, either the assumption of the expandability of the skin was not correct, which I think it is not possible, or the changes on the diagrams regarded to be effect of pulsation have some other causation. It could be caused, for example, by the movement of the finger during the scanning or by some oscillations of some device, for example the scanning system itself. Let's assume the magnification 10x and working distance 20mm, the change $75\mu m$ on image plane represents the movement of the finger towards camera in about $300\mu m$ (see section 4.4.2.2). This value is much higher than the expandability of the finger, but still small enough not to be noticed be human eye. Therefore, I assume that the changes in the sequence have some other reason than pulsation of the human body. I think there were some vibrations presented in the lab during the measurement, or, even simpler, the finger was not still and stable.

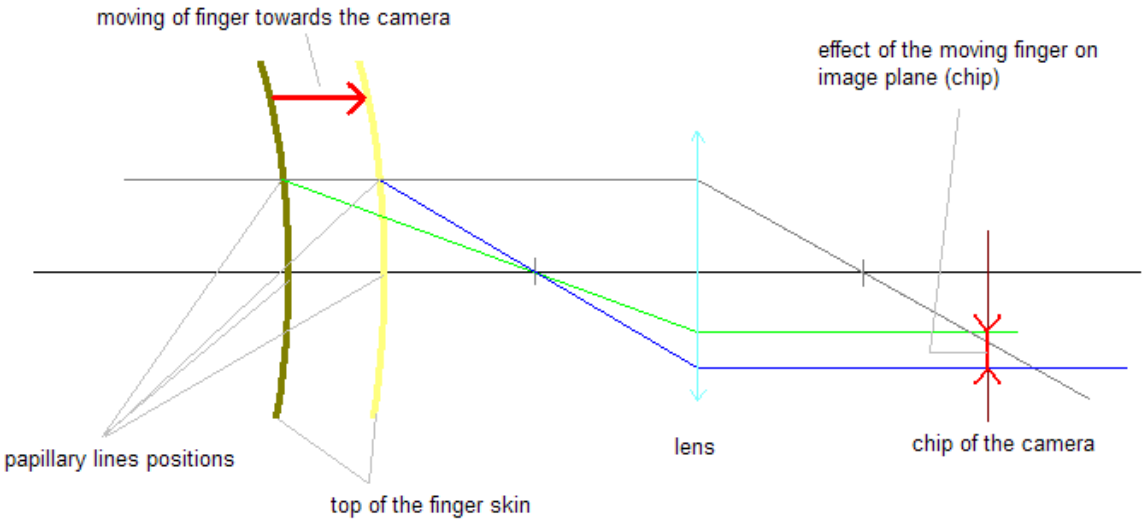

Figure 4.8. Diagram, which shows the effect of movement of the finger on the image plane.

My assumption could be proven by the fact, that the resolution of the image was not high enough to even capture the significant evidence of the expandability of the skin.

The conclusion is following. The assumption, that the change on the diagrams is an effect of pulsation, was probably wrong. There is probably no evidence of pulsation captured on the Peter Dragula's sequences.

The comparison with dummy finger should be done, so the difference between results measured on the live finger and forge finger could be presented.

4.4.2.2 The calculation of the effect of moving finger towards the camera

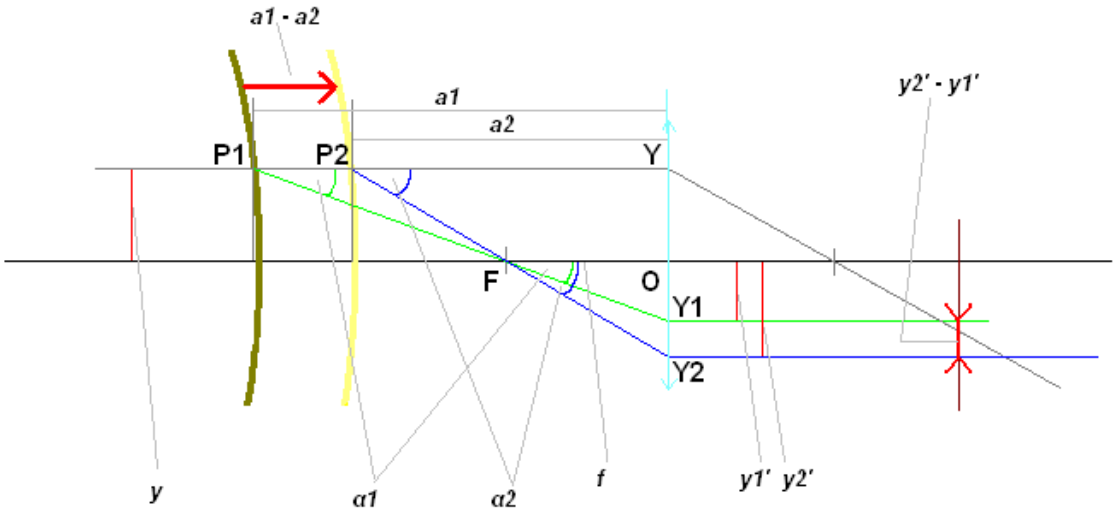

Figure 4.9. The diagram displayed on Figure 4.8 with markings of the sizes

$$\begin{aligned} y_1' &= 75\,px * 5\mu m = 375\mu m \\ y_2' &= 90\,px * 5\mu m = 450\mu m \\ m_1 &= 10 \\ y &= y_1' / m_1 = 37{,}5\mu m \\ m_2 &= \frac{y_2'}{y} = 12 \end{aligned} \tag{4.1}$$

$$a_1 = 2cm = 20mm = 20000\mu m$$

$$\tan\alpha_1 = \frac{y + y_1'}{a_1} = \frac{412{,}5}{20000} = 0{,}020625 \tag{4.2}$$

From the Figure 4.9 we know the sizes of the images. From these values the magnification and object size is calculated (Eq. (4.1)). To calculate the size of change (motion of the finger) we use the similarity of triangles. First we calculate the angle α_1, which the papillary line is seen in one position (Eq. (4.2)). Then the angle α_2 of second position is calculated. From this angle, the distance from the camera a_2 is obtained. Once we know both distance values (a_1, a_2), we know the size of motion.

The exact mathematical calculation is done on the sequence of equations at (4.3) and (4.4). The description of operations is following: the tangent value of angle α_1 is very small, therefore $\tan\alpha_1 \cong \alpha_1$. The same is valid for α_2. The α_1 is calculated from the triangle P_1YY_1 and the α_2 from the triangle P_2YY_2. The angles α_1 and α_2.are also in triangles FOY_1 and FOY_2, respectively. These triangles have the same side *f*, so the α_2.can be expressed by α_1. Once we know the angle in P_2YY_2, we can calculate a_2. Now we know both position of finger during the movement, so we can calculate

the value of this small motion. Vice versa, when we know the size of motion, we know the effect on the chip.

$$\begin{aligned} \alpha_1 \cong \tan\alpha_1 &= 0{,}020625 \\ \tan\alpha_1 = \frac{f}{y_1'} &\Rightarrow f = \alpha_1 * y_1' \\ \tan\alpha_2 = \frac{f}{y_2'} &\Rightarrow f = \alpha_2 * y_2' \\ \frac{y_1'}{\alpha_1} = \frac{y_2'}{\alpha_2} &\Rightarrow \alpha_2 = y_2' \frac{\alpha_1}{y_1'} \\ \alpha_2 = 450 * \frac{0{,}020625}{375} &= 0{,}02475 \end{aligned} \tag{4.3}$$

$$\begin{aligned} &\tan\alpha_2 = \frac{y + y_2'}{a_2} \Rightarrow \\ &\Rightarrow a = \frac{y + y_2'}{\tan\alpha_2} = \frac{37{,}5 + 450}{0{,}02475} = 19697\mu m \\ &a_1 - a_2 = 303\mu m \end{aligned} \tag{4.4}$$

4.4.3 Sequences from Sony camera

First of all I test whether my calculations are correct. A made a snapshot of a ruler, which has proven my assumptions. The values of optical lens system parameters were nearly the same as on first row of Tab. 3.2 and Tab. 3.3. They were not exactly the same, however, the technique of measurement (just a simple ruler was used) could not retrieve better results. From this row we know, that one pixel is about 5,5μm.

I made several sequences from fake and real fingerprint. Both were done in resolution 1280x960 pixels, however, first sets were in GBR24 RAW format, which leads to reduction of effective pixels to half (640x480). The images of fake fingerprint are used to show the amount of noise (disproportions) in still and stable fingerprint. This is done to test, whether the device is able to capture liveness, or it will be lost in noise signal (the changes in noise signal will be stronger than the changes invoked by liveness property). The fake fingerprint is a fingerprint image printed on a foil. Because the background was transparent, white paper was put under the foil. Just a one sample of fake fingerprint was used. The live samples were obtained from my thumb and index finger. Because the thumb is much wider then index finger, the papillary line proportions are wider as well.

First, I present the results from sequences of fake fingerprint. On the first set of images (Figure 5.1) is one threshold image from the sequence with direction line (red) and normal line (green). Direction line represents average direction of all papillary lines in the image and normal line is the direction of the shortest way between two neighbor papillary lines. From the other diagrams just some important are presented in this work, the rest is available on the DVD. The Figure 5.3 shows the

dependency between small (top set of charts) and great (bottom set of charts) changes of average gray value and the distance between two papillary lines. The estimation of noise is done from Figure 5.4, Figure 5.5 and Figure 5.6. On these diagrams could be seen, that the results of average distances and width of papillary lines are changing a little, without any significant influence from the environment. Therefore, this signal is called noise. The size (amplitude) of noise is important to estimate, because it can nullify the effects of liveness.

The first and the second set of chart of Figure 5.6 represent the live finger, the third chart a fake finger. First chart is produced from images captured at resolution 1px = 11µm, second at resolution 1px = 5,5µm and third again at 1px = 11µm. The fake fingerprint was not still, but was slightly moving as real finger, which leads to change of average width of 5pixels, that means 55µm. This is less than in case of live finger, where the values were 10px = 110µm and 8px=44µm, respectively. The average distances between two papillary lines are 50px, 80px and 40px (550µm, 440µm and 440µm, respectively).

Next, on the diagrams Figure 5.2 samples from the sequences of live fingerprint images are presented. Again, the direction line and normal line are displayed.

4.4.4 Conclusions from my sequences

First, before the final conclusion of the liveness detection method is done, we need to eliminate the mistakes during the processing of the images. From the diagrams of fake fingerprint images could be seen, that the estimation (calculation) of direction line and normal line is precise (Figure 5.1). This step is done well. The next step is the threshold estimation. As could be seen on first image of (Figure 5.3), the amount of white pixels after threshold has no effect on the distances in the image. Even the measurement algorithm of distances depends on the quality of the image after threshold, there is no direct dependence between small changes of threshold and distances between papillary lines. That means that some possible mistakes of threshold estimation have no direct effect to distances between papillary lines. (However, greater changes average gray value effects the amount of white pixels and also the width of papillary line). So, the last possible mistake of the algorithm could be in calculation of the distances. This could happen just on the non-averaged distances, because the calculation of average distance has a valid range of distance, which eliminates the noise of the picture after threshold. Therefore, we can say that the processing of the image is correct and we can focus on the results.

First the calculation of the distances will be done, to prove that the measurement is correct. From the images on Figure 5.1 and Figure 5.2 could be seen, that the edges are narrower than valleys, which does not represent the reality. This happens because of illumination angle and threshold. So, just the distances between papillary lines will prove the correctness of measurement. From the Figure 5.3, Figure 5.4 and Figure 5.6 we obtained the distances 418μm, 440μm and 500μm. All these values

are in valid range of width of papillary lines (distance between two papillary lines) as is predicted by Tab. 3.1. Other way to test the correctness of measurement is to count the width of papillary lines from the image from the sequence in pixels. From the Figure 4.10 we obtained the value 107 pixels. The settings 1 from Tab. 3.3 predicted the width of papillary line to be displayed on 127 pixels. The lower value probably means, that the papillary line is narrower than the maximal value (0,7μm), which was used calculations. Therefore we can say that the measurement was correct.

The most important is the estimation of noise amplitude in the sequence of images. As was written earlier, if this value will be too high, it nullifies the effect of liveness. From the Figure 5.4, Figure 5.5 and Figure 5.6 we can deduct the amplitude to be 1,1μm, 5,5μm and higher. This is more than the change of distance between two papillary lines during the pulsation (0,454μm). Therefore, the liveness could not be detected from the images using this method. However, this does not mean that the method is wrong, just the size of change we want to capture is so small, that any other influence of the environment has a stronger effect on the final result. Further, to prove this assumption, I might add, that the 0,454μm is a wavelength of blue light, which is less than red light wavelength. The red is the main color that is reflected by the illuminated finger. To successful capture of any object, at least the wavelength of half size of the object is required. Therefore, to capture the effect of liveness on the finger, we have to use a light of wavelength 0,25μm. This wavelength belongs to ultraviolet light. There will be probably none reflection at all for this wavelength, or just very poor. Also, the acceptance of UV light will probably very low. The conclusion is straight. The liveness detection could not be detected on the changing of distances between two papillary lines.

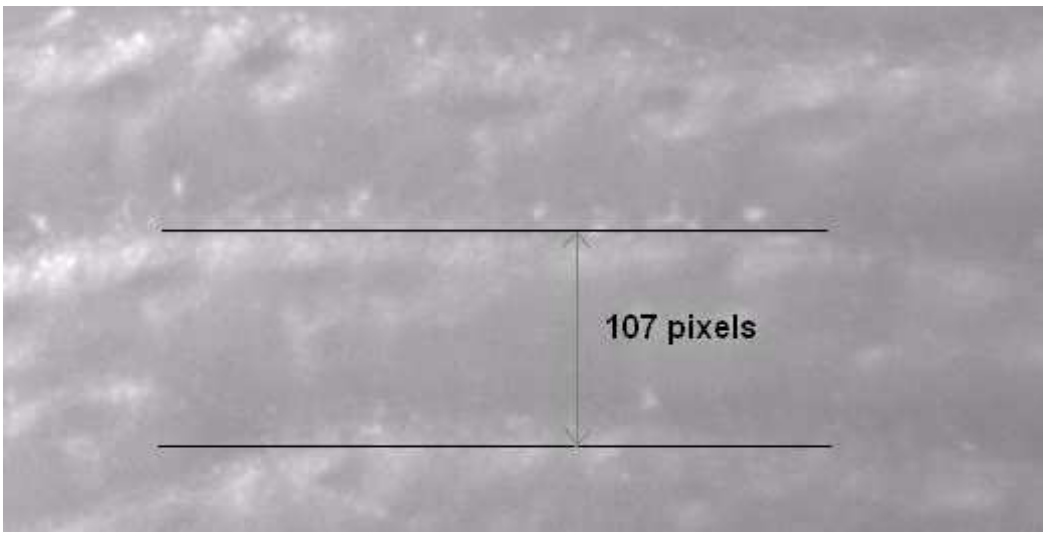

Figure 4.10. The distance between two papillary lines (the width of one papillary line) on one image from sequence of live finger.

However, there is no problem with wavelength when the distances will be measured between more (for example six) papillary lines. On the other hand, the problem with noise still persists.

As was written in introduction, also the liveness detection method based on reflecting a different amount of light was tested on input data. The reflection of light affects the average gray value in the sequence of image. This should lead to significant change of output signal at each pulsation. My pulsation frequency at time of capturing could be between 80 to 120 pulsations per minute. This is 1,5 to 2 pulsations per second. At a frame-rate of 15 frames per second, the effect of pulsation should occur in interval between 10 and 7,5 images. However, no such periodic change was found on results of live fingerprint sequence (Figure 5.6). Therefore, also this method does not lead to liveness detection.

5 Summary

The background about the fingerprint recognition and liveness detection methods was studied and described in chapter 2. The parameters of the optical lens system and macro-objective were calculated in chapter 3 and several possible settings of the parameters were presented (section 3.4.2, Tab. 3.2 and Tab. 3.3). Then the several sequences of the images of fake and live fingerprint were taken (Figure 4.2) in high resolution, even not in the desired. This happens because some parts of capturing device were missing at the time of writing this thesis. The problem was not on our side, because we can not hurry the delivery from the provider of optical system components. Algorithm for analyzing the sequences was presented and tested also on data from previous work by Peter Dragula (Figure 4.1). The results were better and from the first view, the effect of liveness was disclosed. However, after further analysis, this effect was ascribed to the movement of the finger (section 4.4.2). Then the algorithm for processing the sequences was run on my input data. First on a fake fingerprint sequences. It was proven that the results of measurement are correct. From these results the amplitude of noise was estimated. It was proven that this value is higher than the change of distances between two papillary lines due to effect of pulsation, which means the noise nullifies the effect of pulsation on the result images. There was also presented a fact, that the change is so small, that collides with wavelength of blue light, which lead to diffraction of the light and incorrect measurements. Also the changes in amount of light reflected by the skin during the pulsation did not discover the liveness of finger (4.4.4).

The conclusion from these results is following. The expandability can not be measured just between two papillary lines. At least four papillary lines should be scanned to avoid diffraction of the red light, which is the main part of light reflected by the finger. Further, unless the finger will be fixed tightly, which eliminates the noise created by the movement of the finger to the sides or towards the camera, there is no chance to capture such small change as the expandability of the finger during the pulsation is. However the tightly fixing of the finger is questionable, because it could lead to stopping or slowing the circulation of the blood inside the tight part, which would have a negative effect on the expandability. I also think that the resolution of the camera is not enough and higher should be used.

This work proposed the parameters of optical lens system that is necessary to capture the expandability of finger during pulsation. It was also proven, that with present device and measurement conditions the liveness could not be detect and that it might not be detectable at all. For future research in this area I advice to use a camera with higher resolution (at least 3,1Mpx) and to enhance the whole device, especially the place where the finger is scanned.

5.1 The calculation of recommended camera resolution

Now we know, that to avoid the diffraction of the red light, we need to capture the object of size two-times higher than red light wavelength. The top value of red light wavelength is $700nm = 0{,}7\mu m$. Above this value the spectrum comes to infra-red light. Therefore, the object should have at least $1{,}4\mu m$. Let's assume that the object is represented by one pixel on the image. We know that the change per one papillary line is $0{,}454\mu m$. So, the change from two, three and four papillary lines is $0{,}908\mu m$, $1{,}362\mu m$ and $1{,}816\mu m$, respectively. Only the last value is higher than $1{,}4\mu m$, so the object size, that will be displayed on pixel, is $1{,}816\mu m$. The image should then contain four papillary lines in vertical direction, which is $4*700\mu m = 2800\mu m$. This leads to 2800/1,816 = 1542 pixels in vertical direction and 2056 pixel in horizontal direction (if the rate horizontal to vertical is 4 to 3). Therefore, the chip resolution should be 2056x1542 = 3170352 pixels, which is about 3,1 Mpx. Maybe a higher resolution should be recommended, because this calculation assumes the displaying of the object (the expandability of four papillary lines) to one pixel of the image. This is, however, influenced by magnification, which is influenced by additional ring size and multiplication rings. And any size of additional rings can not be guaranteed to buy or construct.

Therefore, let's assume we have only multiplication rings, so we can the set up the magnification only by multiplying the range provided by the lens. The desired magnification for 1/2'' chip with $4{,}65\mu m$ cell size is $4{,}65\mu m/1{,}816\mu m = 2{,}56$x. This, divided by 4, is 0,64x. This value is in range of possible magnifications of Computar lens. So, we can use already bought lens, attach two 2x multiplication rings and buy a new camera with resolution 3,1 Mpx.

5.2 Future work

With a camera of higher resolution, the images with necessary four papillary lines could be captured. Then, after enhancing the fixing of the finger, which would lead to reducing of the noise, new sequences of images could be scanned. In these images the effect of expandability of the skin might be determined. However, this research requires additional finances and a successful result is questionable.

Bibliography

[1] Peter Dragula, Erkennung der feinen Hautbewegungen des Fingers, Diplomarbeit, Brno, FIT VUT, 2007

[2] Anil K. Jain: *Biometric System Security* [online]. [cit. 2008-04-30]. Accessible at WWW: <http://biometrics.cse.msu.edu/Presentations/AnilJain_BiometricsSecurity_Japan_Jan06.pdf>

[3] Geppy Parziale: *Touchless Sensors* [online]. [cit. 2008-04-30]. Accessible at WWW: <http://www.ifingersys.com/Touchless.html>.

[4] KLUZ, Marek: *Liveness testing in biometric system.* Brno: Masaryk University Brno, 2005.

[5] MALTONI, Davide – MAIO, Dario –JAIN, Anil K. – PRABHAKAR, Salil. *Handbook of Fingerprint recognition*. 1. issue. USA: Springer, 2007. 340p. ISBN 0-387-95431-7

[6] Wikipedia. *C mount* [online]. [cit. 2008-04-30]. Accessible at WWW: <http://en.wikipedia.org/wiki/C_mount>.

[7] DRAHANSKY, Martin – NOTZEL, Ralf – FUNK, Wolfgang. *Liveness Detection Based on Fine Movements of the Fingertip Surface*.

[8] Manual, Computar MLH-10x. [cit. 2008-04-30]. Accessible at WWW: <http://www.mengelengineering.dk/PDF/CB/MLH-10X.pdf>.

[9] DRAHANSKY, Martin. *Uvod do biometrickych systemu.*Brno: UITS FIT BUT, 2005.

[10] LODROVA, Dana. *Rozpoznavani zivosti otisku prstu*. Brno, CZ, VUT v Brne, 2007, s. 260-262, ISBN 978-80-214-3408-0

[11] NewScientistTech. *Finger chopped of to beat car security* [online]. [cit. 2008-04-30]. Accessible at WWW: <http://technology.newscientist.com/channel/tech/motoring-tech/mg18624943.600>.

[12] Wikipedia. *Dermis* [online]. [cit. 2008-04-30]. Accessible at WWW: <http://en.wikipedia.org/wiki/Dermis>.

[13] Wikipedia. *Aberration in optical systems* [online]. [cit. 2008-04-30]. Accessible at WWW: <http://en.wikipedia.org/wiki/Aberration_in_optical_systems>.

[14] Wikipedia. Accessible at WWW: <http://www.wikipedia.org>.

[15] SHUCKERS, S. – ABHVANKAR, A.: *Detecting Liveness in Fingerprint Scanners Using Wavelets: Result of the Test Dataset.* Biometric Authentication, Springer, 2004.

[16] DERAKHSHANI, R. – PARTHNASARDI, S. – HORNAK, L. – SHUCKERS, S.: *Perspiration for Detecting Liveness in Fingerprint Scanners – Comparison of Different Classifiers* [online]. [cit. 2008-04-30]. Accessible at WWW: <http://people.clarkson.edu/~biosal/research/perspiration.html>.

[17] PARTHNASARDI, S. – DERAKHSHANI, R. – SHUCKERS, S. – HORNAK, L.: *Spoofing Fingerprint Devices* [online]. [cit. 2008-04-30]. Accessible at WWW: <http://people.clarkson.edu/~biosal/research/spoofingfingerprint.html>.

[18] SHUCKERS, S. - HORNAK, L – NORMAN, T. - DERAKHSHANI, R. – PARTHNASARDI, S.: *Issues for Liveness Detection in Biometrics* [online]. West Virginia University. [cit. 2008-04-30]. Accessible at WWW: <http://www.biometrics.org/html/bc2002_sept_program/2_bc0130_DerakhshabiBrief.pdf>.

[19] THALHEIM, L. - KRISSLER, J. - ZIEGLER, P.: *Body Check, Biometric Access Protection Devices and their Programs Put to the Test in c't magazine.* 11/2002. 114p. Accessible at WWW: <http://www.heise.de/ct/english/02/11/114/>.

[20] PUTTE, T. van der – KEUNING, J.: *Biometrical Fingerprint Recognition: Don't get your fingers burned.* IFIP TC8/WG8.8 Fourth Working Conference on Smart Card Research and Advanced Applications, 289-303p., Kluwer Academic Publishers, 2000. Accessible at WWW: <http://www.keuning.com/biometry/Biometrical_Fingerprint_Recognition.pdf>.

[21] *FTIR.gif* [online].[cit. 2008-04-30]. Accessible at WWW: <http://www.diniro.net/fabbblog/FTIR.gif>.

[22] *Sensing_capacitive_direct.gif* [online]. [cit. 2008-04-30]. Accessible at WWW: <http://pagesperso-orange.fr/fingerchip/biometrics/types/fingerprint/physics/sensing_capacitive_direct.gif>.

[23] STUCKER, M. – GEIL. M. – KYECK, S. – HOFFMAN, K. – ROCHLING, A. – MEMMEL, U. – ALTMEYER, P.: *Interpapillary lines – the variable part of human fingerprint* [online]. Published 2001-07-01. [cit. 2008-04-30]. ISSN 0022-1198. Accessible at WWW: <http://www.astm.org/JOURNALS/FORENSIC/PAGES/JFS4640857.htm>.

[24] Wikipedia. *Zeiss formula* [online]. [cit. 2008-04-30]. Accessible at WWW: <http://en.wikipedia.org/wiki/Zeiss_formula>.

[25] Wikipedia. *Chromatic Abberation* [online]. [cit. 2008-04-30]. Accessible at WWW: <http://en.wikipedia.org/wiki/Chromatic_Abberation>.

[26] REHOR, Martin. *Opticke pristroje.* Skripta. University of Defense, CZ.

[27] Wikipedia. *Lens mount* [online]. [cit. 2008-04-30]. Accessible at WWW: <http://en.wikipedia.org/wiki/Lens_mount>.

[28] *Computar Macro zoom lens MLH-10X* [online]. [cit. 2008-04-30]. Accessible at WWW: <http://www.apisc.com/computar_macro_zoom_lens.htm>.

[29] MATSUMOTO, Tsutomu – MATSUMOTO, Hiroyuki – YAMADA, Koji – HOSHINO, Satoshi: *Impact of Artificial "Gummy" Fingers on Fingerprint System* [online]. [cit. 2008-05-05]. Accessible at WWW: <http://cryptome.org/gummy.htm>.

[30] International Biometric Group: *Biometrics Market and Industry Report 2007-2012* [online]. [cit. 2008-05-05]. Accessible at WWW: <http://www.biometricgroup.com/reports/public/market_report.html>.

[31] Biometrics: *Fingerprint sensing techniques* [online]. [cit. 2008-05-05]. Accessible at WWW: <http://pagesperso-orange.fr/fingerchip/biometrics/types/fingerprint_sensors_physics.htm>.

[32] Optel: *Fingerprint structure imaging based on a ultrasonic camera* [online]. [cit. 2008-05-05]. Accessible at WWW: <http://www.optel.pl/article/english/article.htm>.

[33] *Intergumentary systems* [online] [cit 2008-05-25]. Accessible at WWW: <http://www.mc.vanderbilt.edu/histology/labmanual2002/labsection2/Integumentarysystem03.htm>

[34] Aegis, Electronic Group, Inc: *SONY XCD*-910CR [online]. [cit. 2008-05-25]. Accessible at WWW: <http://www.aegis-elec.com/products/sonyxcdsx910cr.html>

List of terms

Artificial	- fake, fraudulent
BioSAL	- Biomedical Signal Analysis Laboratory at Clarkson University a West Virginia University in USA
BS	- Biometric System
CCD	- Charge-Coupled Device – device used to capture images, usually used in cameras.
CMOS	- Complementary Metal Oxid Semiconductor – device used to capture images (as CCD). CMOS is newer technology than CCD and produces better images.
CoC	- Circle of Confusion
Dactyloscopy	- knowledge about papillary lines. It is being used in criminalistics for identification of persons.
Dermis	- the skin layer under epidermis. Contains papillae, which effect the creation of papillary lines in epidermis.
Epidermis	- the top layer of skin; layer with the papillary lines.
Fiber	- a group of connected cells in an organism with the same function (e.g. muscle fiber)
Imposter	- attacker (of the BS)
Liveness detection	- used in Biometric terminology, means detection of being live, real.
Pulse oxymeter	- a common medical device used to measure body pulse frequency and saturation of blood with oxygen. The measurement is taken usually at the finger.

List of appendices

Appendix 1: Results

Appendix 2: DVD with source codes, all results and diploma thesis in electronic format.

Appendix 1 – Results

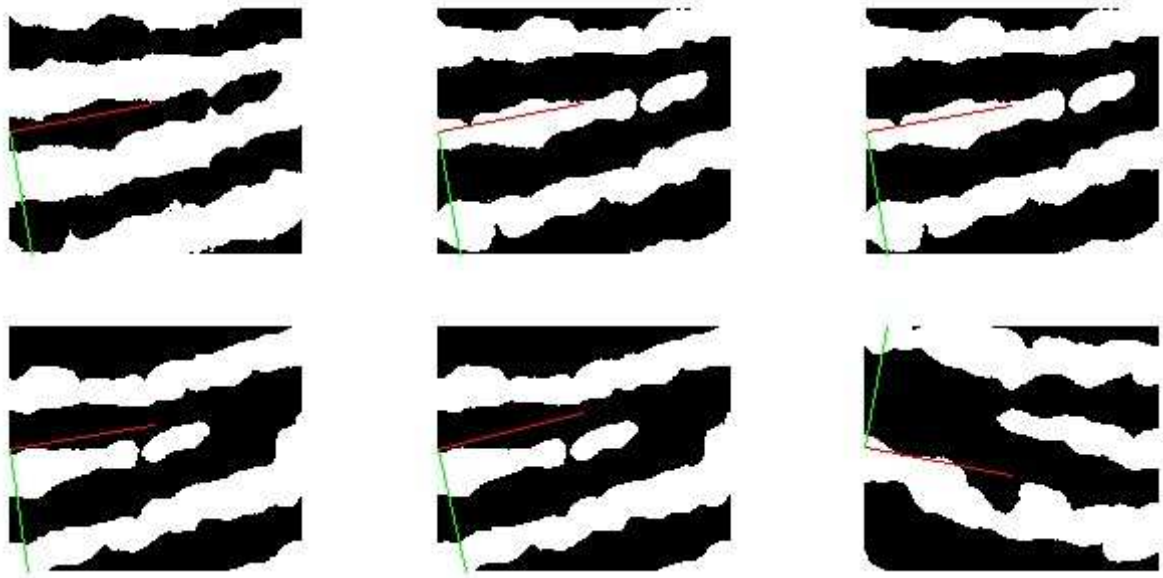

Figure 5.1. Display of direction line (red) and normal line (green) on a sample from several sequences of a fake fingerprint images.

Figure 5.2. Display of direction line (red) and normal line (green) on a sample from several sequences of a live fingerprint images.

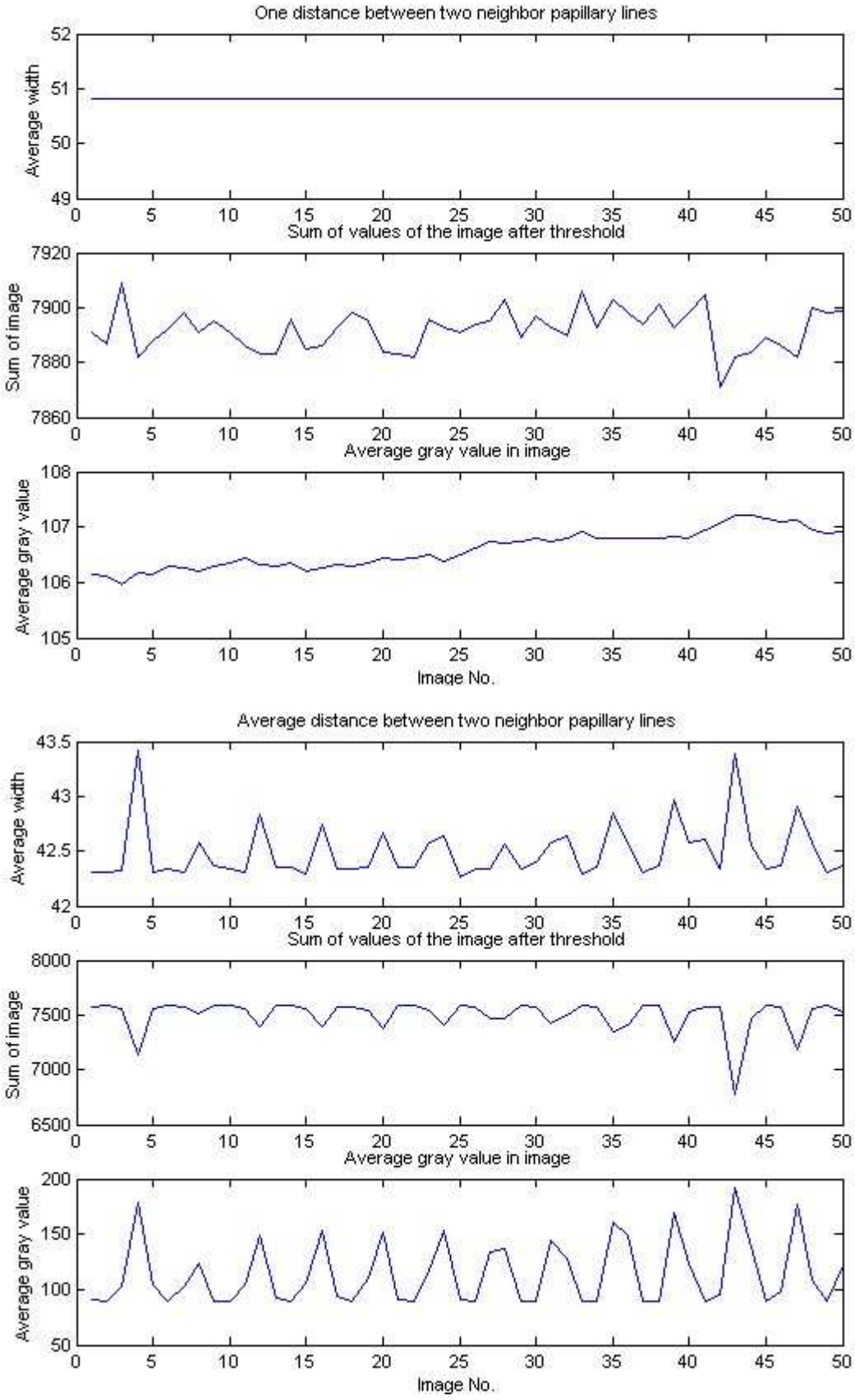

Figure 5.3. Diagrams show the dependency between changes (small and great) to the average gray value and the sum of white pixels after threshold.

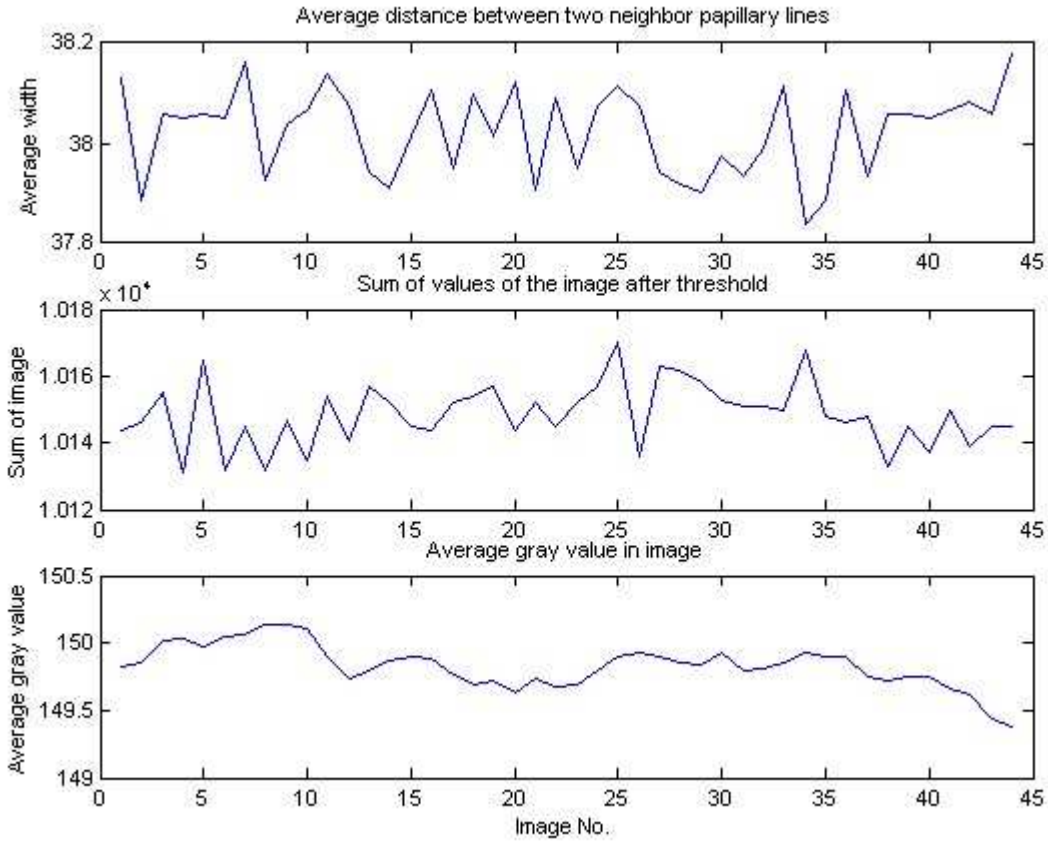

Figure 5.4. On the first chart of the diagram the noise is presented. The maximal value of the noise is 0,4 pixels, which is 4,4µm (at resolution 1px = 11µm). The average distance between two papillary lines is 38px, which is 418µm.

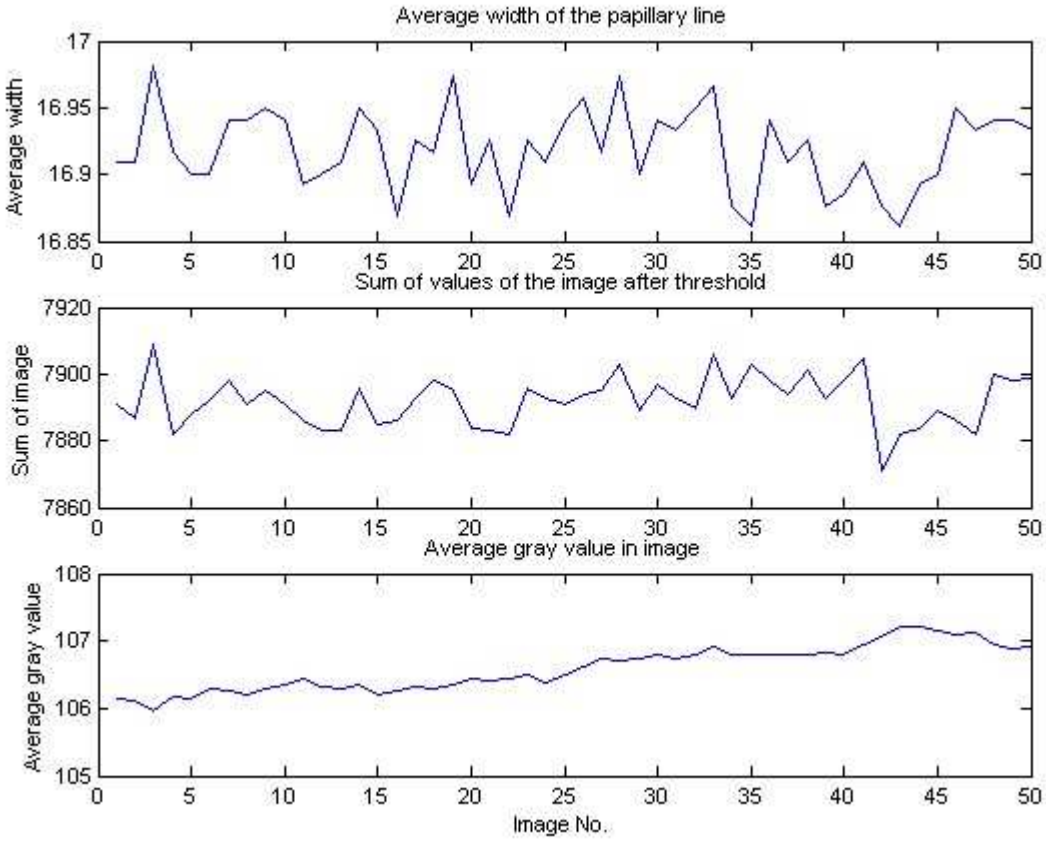

Figure 5.5. The diagram shows, that there are no dependences between small changes of the average width of the papillary lines and the amount of white pixels after threshold or average gray value in the image. (1px=11µm).

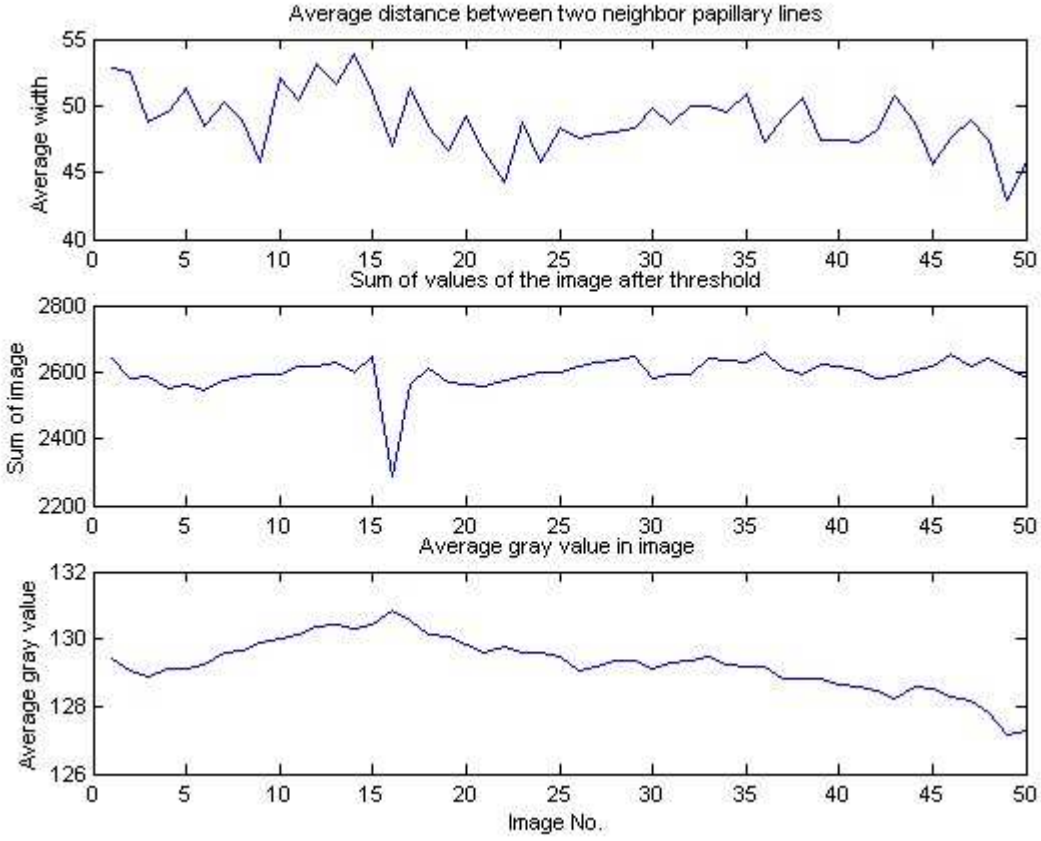
Average distance between two neighbor papillary lines
Average width
Sum of values of the image after threshold
Sum of image
Average gray value in image
Average gray value
Image No.

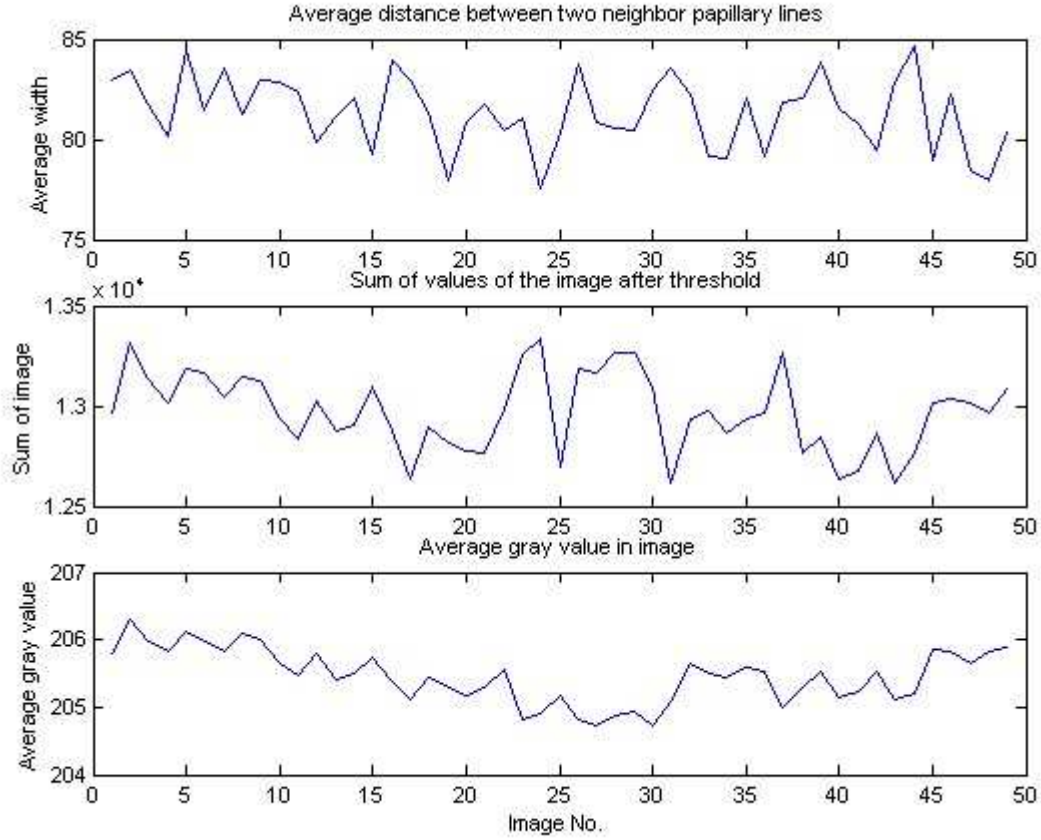
Average distance between two neighbor papillary lines
Average width
Sum of values of the image after threshold
x 10^4
Sum of image
Average gray value in image
Average gray value
Image No.

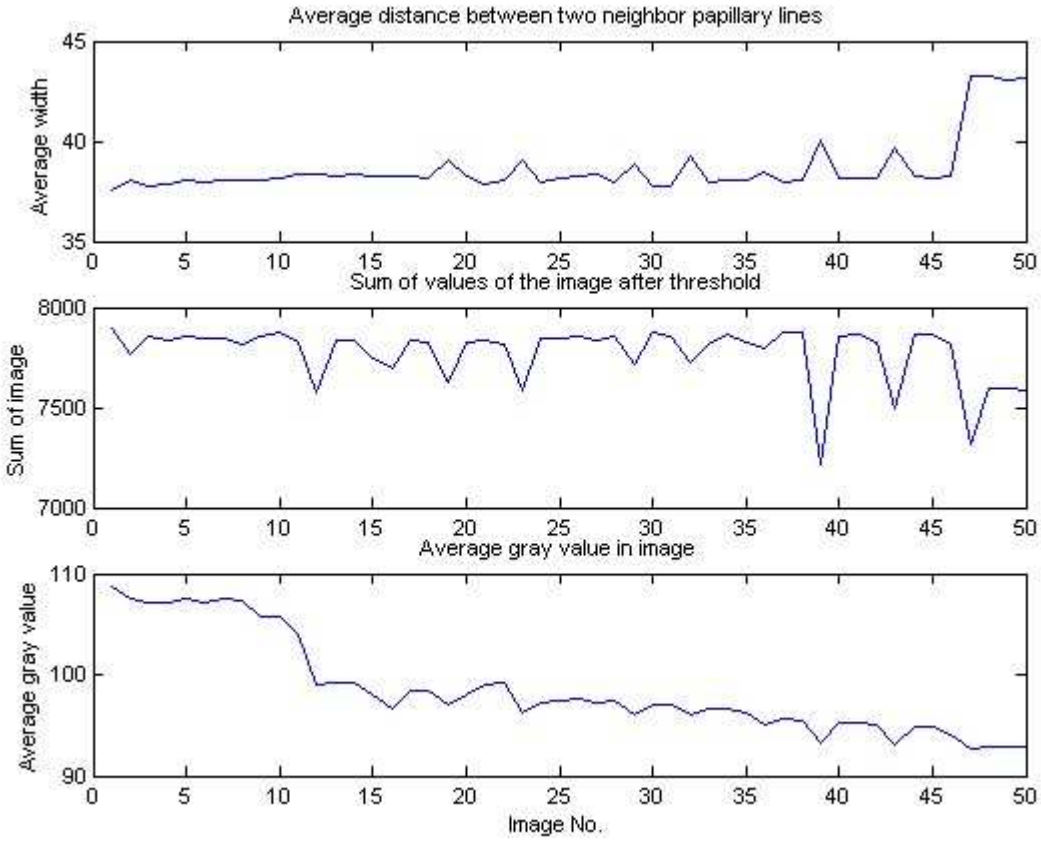

Figure 5.6. Three diagrams to compare the average distance between two neighbor papillary lines.